The potential of carbonyl sulfide as a proxy for gross primary production at flux tower sites

J. M. Blonquist Jr.,[1] S. A. Montzka,[2] J. W. Munger,[3] D. Yakir,[4] A. R. Desai,[5] D. Dragoni,[6] T. J. Griffis,[7] R. K. Monson,[8] R. L. Scott,[9] and D. R. Bowling[1]

Received 29 March 2011; revised 23 August 2011; accepted 27 August 2011; published 15 November 2011.

[1] Seasonal dynamics of atmospheric carbonyl sulfide (OCS) at regional and continental scales and plant OCS exchange at the leaf level have shown a close relationship with those for CO_2. CO_2 has both sinks and sources within terrestrial ecosystems, but the primary terrestrial exchange for OCS is thought to be leaf uptake, suggesting potential for OCS uptake as a proxy for gross primary production (GPP). We explored the utility of OCS uptake as a GPP proxy in micrometeorological studies of biosphere-atmosphere CO_2 exchange by applying theoretical concepts from earlier OCS studies to estimate GPP. We partitioned measured net ecosystem exchange (NEE) using the ratio of measured vertical mole fraction gradients of OCS and CO_2. At the Harvard Forest AmeriFlux site, measured CO_2 and OCS vertical gradients were correlated and were related to NEE and GPP, respectively. Estimates of GPP from OCS-based NEE partitioning were similar to those from established environmental regression techniques, providing evidence that OCS uptake can potentially serve as a GPP proxy. Measured vertical CO_2 mole fraction gradients at five other AmeriFlux sites were used to project anticipated vertical OCS mole fraction gradients to provide indication of potential OCS signal magnitudes at sites where no OCS measurements were made. Projected OCS gradients at sites with short canopies were greater than those in forests, including measured OCS gradients at Harvard Forest, indicating greater potential for OCS uptake as a GPP proxy at these sites. This exploratory study suggests that continued investigation of linkages between OCS and GPP is warranted.

Citation: Blonquist, J. M., Jr., S. A. Montzka, J. W. Munger, D. Yakir, A. R. Desai, D. Dragoni, T. J. Griffis, R. K. Monson, R. L. Scott, and D. R. Bowling (2011), The potential of carbonyl sulfide as a proxy for gross primary production at flux tower sites, *J. Geophys. Res.*, *116*, G04019, doi:10.1029/2011JG001723.

1. Introduction

[2] The difference between gross primary production (GPP) and total ecosystem respiration (TER) equals net ecosystem exchange of CO_2 (NEE), a commonly measured flux at eddy covariance tower sites across the globe [*Baldocchi et al.*, 2001]. Investigation of GPP and TER provides important process-based information about biosphere-atmosphere carbon exchange. Unfortunately, GPP and TER cannot be measured directly during the daytime by eddy covariance and must be estimated using additional information from measurements and models. There are several methods available to estimate GPP and TER from NEE, including regression of nocturnal NEE with environmental driving variables (usually temperature) and extrapolation to daytime [*Goulden et al.*, 1996; *Reichstein et al.*, 2005]; prediction of TER from light response models [*Lasslop et al.*, 2010; *Yi et al.*, 2004]; scaling-up measurements made in leaf, stem, and soil chambers [*Lavigne et al.*, 1997; *Law et al.*, 1999; *Zha et al.*, 2007]; calculation from ecosystem process models [*Baldocchi and Wilson*, 2001; *Ogée et al.*, 2003a; *Sacks et al.*, 2007]; and stable isotope approaches [*Ogée et al.*, 2003b; *Zobitz et al.*, 2008]. New methods are also emerging; for example, correlation analysis based on flux variance similarity [*Scanlon and Kustas*, 2010]. The most common NEE partitioning approach is to estimate TER using a regression of NEE on turbulent nights (assumed equal to TER) against temperature, then extrapolation of the TER-temperature relationship to daytime periods, where GPP is then calculated as NEE minus TER [*Reichstein et al.*, 2005].

[1]Department of Biology, University of Utah, Salt Lake City, Utah, USA.
[2]Global Monitoring Division, NOAA Earth System Research Laboratory, Boulder, Colorado, USA.
[3]Department of Earth and Planetary Sciences, Harvard University, Cambridge, Massachusetts, USA.
[4]Department of Environmental Sciences and Energy Research, Weizmann Institute of Science, Rehovot, Israel.
[5]Department of Atmospheric and Oceanic Sciences, University of Wisconsin-Madison, Madison, Wisconsin, USA.
[6]Department of Geography, Indiana University, Bloomington, Indiana, USA.
[7]Department of Soil, Water, and Climate, University of Minnesota-Twin Cities, St. Paul, Minnesota, USA.
[8]Department of Ecology and Evolutionary Biology, University of Colorado at Boulder, Boulder, Colorado, USA.
[9]Southwest Watershed Research Center, USDA ARS, Tucson, Arizona, USA.

0148-0227/11/2011JG001723

[3] Challenges and often large uncertainties are associated with each NEE partitioning method. For example, low nighttime turbulence and advection fluxes can result in problematic NEE measurements and make regression-based estimates uncertain [*van Gorsel et al.*, 2009], light response models do not capture within-day variability [*Reichstein et al.*, 2005], chamber measurements require scaling to represent the entire ecosystem [*Lavigne et al.*, 1997], and stable isotope approaches are dependent on isotopic disequilibrium between GPP and TER, which is sometimes difficult to resolve [*Ogée et al.*, 2004]. Additionally, different NEE partitioning methods provide different estimates of GPP and TER, leading to fundamental uncertainty about the process of interest [*Desai et al.*, 2008; *Griffis et al.*, 2004; *Lasslop et al.*, 2010; *Stoy et al.*, 2006]. Independent, measurement-based approaches to estimate GPP and TER are required.

[4] Recent studies have suggested the utility of carbonyl sulfide (OCS) uptake as a proxy for GPP, based on the close relationship between seasonal dynamics of OCS and CO_2 mole fractions at regional and continental scales [*Blake et al.*, 2008; *Campbell et al.*, 2008; *Montzka and Tans*, 2004; *Montzka et al.*, 2007; *Sandoval-Soto et al.*, 2005] and the link between OCS and CO_2 uptake at the leaf level [*Seibt et al.*, 2010; *Stimler et al.*, 2010a]. OCS is the most abundant reduced sulfur gas in the atmosphere, with mole fractions ranging from approximately 300–550 pmol mol^{-1} (pptv) near the surface, depending on season, and a global mean of approximately 500 pmol mol^{-1} [*Montzka et al.*, 2007]. The tropospheric lifetime of OCS is relatively long, 2–4 years [*Montzka et al.*, 2007; *Suntharalingam et al.*, 2008], and the major OCS sinks are vegetation, soils, reaction with oxidizing radicals in the troposphere and stratosphere, and photolysis in the stratosphere; the major sources are oceans, volcanic eruptions, and anthropogenic emissions (e.g., biomass burning, coal-fired power plants, and certain industrial processes) [*Watts*, 2000]. Seasonal variation in the northern hemisphere is largely influenced by terrestrial vegetation uptake, while variation in the southern hemisphere is largely influenced by oceanic fluxes [*Kettle et al.*, 2002; *Montzka et al.*, 2007]. Studies of OCS aimed at understanding exchange in terrestrial ecosystems have measured OCS exchange in soils [*Castro and Galloway*, 1991; *Kesselmeier et al.*, 1999; *Liu et al.*, 2010; *Simmons et al.*, 1999; *Steinbacher et al.*, 2004; *Van Diest and Kesselmeier*, 2008] and vegetation [*Brown and Bell*, 1986; *Goldan et al.*, 1988; *Kesselmeier and Merk*, 1993; *Kluczewski et al.*, 1985; *Sandoval-Soto et al.*, 2005; *Yonemura et al.*, 2005].

[5] The few flux tower-scale OCS studies that have been conducted suggest linkage to GPP [*Bartell et al.*, 1993; *Mihalopoulos et al.*, 1989; *Mihalopoulos and Nguyen*, 2001; *White et al.*, 2010; *Xu et al.*, 2002], and thereby potential for OCS uptake as a proxy for GPP. Our goal is to explore the utility of OCS measurements as a means of quantitatively estimating GPP in micrometeorological studies. In the following theory section we provide a summary of relevant studies, including those conducted at the flux tower scale, and develop the theoretical framework to estimate GPP from OCS measurements. Then, we present measured vertical OCS mole fraction gradients from a temperate deciduous forest (Harvard Forest AmeriFlux site) and use them to estimate GPP by partitioning measured NEE (from eddy covariance). These GPP estimates are compared to GPP estimates from a widely used NEE partitioning method [*Reichstein et al.*, 2005]. Finally, we evaluate the potential of OCS measurements for estimating GPP at other AmeriFlux sites, where OCS was not measured, by deriving vertical OCS mole fraction gradients from CO_2 mole fraction profile measurements, and analyzing the relationship to GPP.

2. OCS as a Proxy for GPP: Available Evidence and Theory

[6] While the OCS studies that have been conducted suggest the possibility of OCS uptake as a GPP proxy, to our knowledge no studies have yet estimated GPP from OCS measurements. The following requirements (1–4) should be met for OCS uptake to be used as a GPP proxy at the flux tower scale (land surface area of 10^2–10^6 m^2): (1) OCS and CO_2 must diffuse along the same physical pathway from the atmosphere through stomata to the point in leaves where the first biochemical step of metabolism of the gases takes place [*Stimler et al.*, 2010a]. (2) OCS exchange must be a one-way flux from the atmosphere to leaves (no OCS compensation point or OCS release analogous to respiratory release of CO_2) [*Stimler et al.*, 2010a]. (3) OCS and CO_2 cannot directly or indirectly interact (no inhibitory/toxicity effects between the gases) [*Stimler et al.*, 2010a]. (4) Any other OCS fluxes within the ecosystem must be negligible compared to plant uptake [*Campbell et al.*, 2008; *Montzka et al.*, 2007].

[7] In vitro studies of plant enzyme uptake of OCS have provided support for requirement 2. *Protoschill-Krebs and Kesselmeier* [1992] showed that carbonic anhydrase (CA), PEP-C, and Rubisco can metabolize OCS, with the key enzyme being CA, which irreversibly hydrates OCS to form CO_2 and hydrogen sulfide (H_2S) [*Notni et al.*, 2007]. *Protoschill-Krebs et al.* [1996] found the affinity of CA for OCS was approximately 1,000 times greater than that for CO_2, with a strong linear relationship between CA and OCS consumption.

[8] Leaf level gas exchange studies have provided support for requirements 1–3. *Stimler et al.* [2010a] studied three C_3 species and found stomatal conductance to OCS in the dark was significantly reduced relative to in the light, and stomatal conductance to and assimilation of OCS were significantly reduced following fumigation with abscisic acid, demonstrating stomatal control of OCS exchange. *Stimler et al.* [2010a] also reported that emissions of OCS were not detectable when leaves were exposed to OCS-free air in the light, indicating there was no OCS release, nor compensation point. Additionally, they found that OCS uptake remained constant at elevated levels of CO_2, and similarly, CO_2 uptake remained constant at elevated levels of OCS, indicating there were no apparent cross interactions or inhibitory/toxicity effects between CO_2 and OCS within the mole fraction ranges tested. However, competitive inhibition of CA by CO_2 was found during OCS and CO_2 gas exchange measurements in decaying leaf litter [*Kesselmeier and Hubert*, 2002], indicating this possibility in live plant leaves exists. Results from *Stimler et al.* [2010a] were consistent with leaf level results from *Sandoval-Soto et al.* [2005], who studied four other C_3 species, and found that (1) OCS uptake was highly correlated to CO_2 uptake and stomatal conductance to CO_2, (2) OCS uptake closely followed the light/dark cycle, and (3) CO_2 and OCS uptake rapidly declined to near zero following

application of abscisic acid, all indicating OCS uptake occurred predominantly through stomata. *Sandoval-Soto et al.* [2005] also found OCS emission did not occur, even at low ambient OCS, indicating a minimal-to-negligible OCS compensation point.

[9] The few OCS studies at the flux tower scale have provided support for requirements 1–3. *Bartell et al.* [1993] estimated OCS flux from a wet meadow and found it followed a diel pattern (with maximum uptake near midday and near-zero exchange at night) and was related to CO_2 flux, water vapor flux, and photosynthetically active radiation (PAR), indicating stomatal control of OCS uptake. Results from *Xu et al.* [2002], who measured OCS flux over a spruce forest (with relaxed eddy accumulation), were consistent and showed that during the day the forest was an OCS sink; OCS flux was also related to PAR, CO_2 flux, and water vapor flux.

[10] Soil is a major component of terrestrial ecosystems and may influence OCS exchange at the flux tower scale, while OCS fluxes from oceans, volcanic eruptions, reaction with oxidizing radicals, and anthropogenic emissions are likely to be minor (data from *White et al.* [2010] indicate the possibility of oceanic effects). Soil microbes contain CA [*Wingate et al.*, 2009] and may assimilate and act as a sink for OCS. Additionally, soil OCS uptake has been shown to be dependent on soil physical properties [*Van Diest and Kesselmeier*, 2008]. Most studies have shown soils are OCS sinks when ambient air is injected into the flux chamber rather than OCS-free air [*Castro and Galloway*, 1991; *Geng and Mu*, 2004; *Kesselmeier et al.*, 1999; *Kuhn et al.*, 1999; *Mihalopoulos and Nguyen*, 2001; *Simmons et al.*, 1999; *Steinbacher et al.*, 2004; *Van Diest and Kesselmeier*, 2008; *White et al.*, 2010], with the exception of paddy soils [*Liu et al.*, 2010]. However, soil OCS uptake appears to be small relative to vegetation uptake, providing support for requirement 4. Vertical profile measurements of OCS over various ecosystems have shown significant near-surface drawdown, compared to above-canopy heights, indicating a surface OCS sink [*Bartell et al.*, 1993; *Mihalopoulos et al.*, 1989; *Mihalopoulos and Nguyen*, 2001; *White et al.*, 2010], with minor soil uptake compared to vegetation and/or ecosystem uptake [*Mihalopoulos and Nguyen*, 2001; *White et al.*, 2010]. *Steinbacher et al.* [2004] measured soil uptake in a spruce forest using surface chambers, and found OCS uptake was less than 1% of total ecosystem OCS flux (total ecosystem flux was measured above the canopy by *Xu et al.* [2002]), indicating uptake was dominated by vegetation. Results from *White et al.* [2010] for a loblolly pine forest were consistent with those of *Steinbacher et al.* [2004], as soil OCS uptake measured with surface chambers was less than 5% of estimated daytime uptake by vegetation (inferred from branch enclosures).

[11] There are some flux tower scale studies that suggest complications to using OCS as a proxy for GPP. Daytime measurements of above-canopy OCS flux made by *Xu et al.* [2002] showed uptake by a spruce forest, but nocturnal emission (when GPP was zero). Thus, it is possible that OCS uptake measured during the day was a net flux representing the balance between OCS uptake and emission, violating requirement 4. Vertical profile measurements of OCS have also indicated emission from a loblolly pine forest [*Berresheim and Vulcan*, 1992]. Emission of organic sulfur compounds from a forest canopy has been reported [*Puxbaum and König*, 1997], but emission of OCS from a loblolly pine forest is puzzling in light of recent results from *White et al.* [2010], who found loblolly pine trees were an OCS sink, even at night when trees were not photosynthesizing. This phenomenon was thought to be due to nonzero nocturnal stomatal conductance in loblolly pines [*Caird et al.*, 2007], resulting in nocturnal OCS uptake because CA activity is light independent [*Protoschill-Krebs et al.*, 1996]. This does not necessarily impact the use of OCS measurements as a GPP proxy, as GPP is zero at night. More work is required to determine the ecosystems in which OCS exchange is dominated by vegetation and the extent to which other fluxes are nonnegligible.

[12] When requirements 1–4 are satisfied, OCS measurements can be used to directly estimate GPP at the flux tower scale via one of two methods: (1) OCS flux measurements or (2) simultaneous OCS and CO_2 vertical gradient measurements. The first method is fully independent of NEE measurements, but requires (1) direct measurement of OCS fluxes (ideally by eddy covariance), (2) ambient CO_2 and OCS mole fraction measurements, and (3) incorporation of the leaf level uptake relationship between OCS and CO_2, defined as leaf relative uptake (LRU) [*Sandoval-Soto et al.*, 2005]

$$\mathrm{GPP} = \mathrm{F_{OCS}}\left(\frac{\mathrm{C_{aCO2}}}{\mathrm{C_{aOCS}}}\right)\left(\frac{1}{\mathrm{LRU}}\right) \tag{1}$$

where F_{OCS} is OCS flux (pmol m^{-2} s^{-1}), C_{aCO2} is ambient CO_2 mole fraction (μmol mol^{-1}), and C_{aOCS} is ambient OCS mole fraction (pmol mol^{-1}). LRU is calculated by dividing the normalized leaf level OCS flux (mol m^{-2} s^{-1}) by the normalized leaf level CO_2 flux (mol m^{-2} s^{-1}), where normalized fluxes are measured fluxes divided by OCS and CO_2 mole fractions, respectively. *Sandoval-Soto et al.* [2005] used equation (1) to estimate the global OCS sink from GPP estimates. *Campbell et al.* [2008] used equation (1) and an atmospheric transport model to simulate vertical atmospheric OCS profiles over land in the northern hemisphere and found measured and modeled OCS profiles agreed, indicating OCS drawdown in the troposphere was likely driven primarily by GPP.

[13] The second method to estimate GPP does not require direct OCS flux measurements, but requires (1) NEE measurements, (2) OCS and CO_2 vertical gradient measurements, and (3) LRU. This method will only work when gradients can be analytically measured. The ratio of GPP to NEE is proportional to the relative gradient of OCS (RG_{OCS}) (m^{-1}) divided by the relative gradient of CO_2 (RG_{CO2}) (m^{-1}), defined as ecosystem relative uptake (ERU) [*Campbell et al.*, 2008]

$$\mathrm{RG_{OCS}} = \frac{\mathrm{G_{OCS}}}{\mathrm{C_{aOCS}}} \tag{2}$$

$$\mathrm{RG_{CO2}} = \frac{\mathrm{G_{CO2}}}{\mathrm{C_{aCO2}}} \tag{3}$$

$$\mathrm{ERU} = \frac{\mathrm{RG_{OCS}}}{\mathrm{RG_{CO2}}} \tag{4}$$

$$\frac{\mathrm{GPP}}{\mathrm{NEE}} = \mathrm{ERU}\left(\frac{1}{\mathrm{LRU}}\right) \tag{5}$$

where RG_{OCS} (m^{-1}) and RG_{CO2} (m^{-1}) at the flux tower scale are near- or within-canopy OCS and CO_2 mole fraction gradients, G_{OCS} (pmol mol^{-1} m^{-1}) and G_{CO2} (μmol mol^{-1} m^{-1}), respectively, normalized by C_{aOCS} and C_{aCO2}. Rearrangement of equation (5) shows that the ratio of the relative vertical mole fraction gradients, ERU, is proportional to GPP/NEE scaled by the ratio of relative leaf exchange rates, LRU. We stress that gradients are not used to determine fluxes here, only to scale NEE to GPP. Thus, the ratio of relative uptakes, ERU/LRU, is used to scale a measured flux, NEE (from eddy covariance), to a related flux, GPP. Hence, problems associated with within-canopy gradient measurements and countergradient fluxes [*Cellier and Brunet*, 1992; *Denmead and Bradley*, 1985; *Raupach*, 1979] are not critical limitations in this application. Aircraft measurements over the midwestern U.S. over multiple years have revealed a mean ERU for North America of between 5 and 6 during June–August, suggesting that on a relative basis net OCS uptake during summer is 5–6 times greater than net CO_2 uptake [*Campbell et al.*, 2008; *Montzka et al.*, 2007]. This feature results from uptake of both gases primarily by vegetation, with the influence of two offsetting processes affecting CO_2 but not OCS: back diffusion of CO_2 out of leaves after it has been reversibly hydrated by CA [*Notni et al.*, 2007; *Stimler et al.*, 2010a], characterized by LRU, and release of CO_2 via cellular respiration, characterized by GPP/NEE.

[14] Estimation of GPP via either method requires that LRU be measured or estimated. Leaf level fluxes and mole fractions can be directly measured, but leaf CO_2 and OCS exchange measurements are time and labor intensive and are rarely made in the field. An alternative to direct measurement was proposed by *Seibt et al.* [2010]

$$\mathrm{LRU} = \frac{\left(1 - \frac{C_{mOCS}}{C_{aOCS}}\right)}{R_{CO2-OCS}\left(1 + \frac{g_{sOCS}}{g_{iOCS}}\right)\left(1 - \frac{C_{iCO2}}{C_{aCO2}}\right)} \tag{6}$$

where C_{mOCS} is mole fraction of OCS in mesophyll cells (pmol mol^{-1}), C_{iCO2} is mole fraction of CO_2 in leaf intercellular air spaces (μmol mol^{-1}), $R_{CO2\text{-}OCS}$ is the ratio of binary diffusivities (in air) of CO_2 and OCS (approximately 1.2 [*Seibt et al.*, 2010]), g_{sOCS} is stomatal conductance to OCS (mol m^{-2} s^{-1}), and g_{iOCS} is internal conductance to OCS (mol m^{-2} s^{-1}) (conductance from leaf intercellular air spaces to mesophyll cells). *Seibt et al.* [2010] derived equation (6) on the basis of a shared diffusion pathway for OCS and CO_2 and a model for leaf OCS uptake analogous to gradient-based models for leaf water loss and CO_2 uptake. Conceptually separate diffusion endpoints for CO_2 and OCS were assumed in the derivation; CO_2 diffusion in air was terminated at leaf intercellular air spaces, but continues in liquid to the site of Rubisco; OCS diffusion was terminated inside mesophyll cells, at the hypothesized site of CA. As *Seibt et al.* [2010] indicated, the spatial distribution of CA is not known. However, they hypothesized a location upstream of Rubisco, inside mesophyll cells and directly adjacent to intercellular spaces, and considered this to be the actual endpoint for OCS. From this hypothesis, *Seibt et al.* [2010] simplified equation (6) by assuming that g_{iOCS} is much larger than g_{sOCS} and that C_{mCOS} was zero, based on observations that OCS emission does not occur [*Sandoval-Soto et al.*, 2005; *Stimler et al.*, 2010a].

[15] Estimates of g_{sOCS}/g_{iOCS} and C_{mOCS}/C_{aOCS} are required to estimate LRU from equation (6). Based on OCS and CO_2 exchange measurements in C_3 leaves, *Stimler et al.* [2010a] provided estimates of gas mole fractions and conductances at each point along the OCS and CO_2 diffusion pathway from ambient air to leaf chloroplasts. They assumed the chloroplast surface inside mesophyll cells was the endpoint for OCS, and found that the OCS mole fraction at the chloroplast surface was near 40 pmol mol^{-1}, yielding C_{mOCS}/C_{aOCS} of approximately 0.08 (ambient OCS mole fraction was near 500 pmol mol^{-1}), rather than zero as assumed by *Seibt et al.* [2010]. *Stimler et al.* [2010a] also found g_{sOCS}/g_{iOCS} was approximately 0.2. When values of $C_{mOCS}/C_{aOCS} = 0.08$ and $g_{sOCS}/g_{iOCS} = 0.2$ were entered in equation (6), LRU ranged from 1.3–3.2 for a C_{iCO2}/C_{aCO2} range of 0.5–0.8 (Figure 1; see also Figure 3 of *Seibt et al.* [2010]), which approximately spans C_3 ecosystems [*Seibt et al.*, 2010]. Other values of C_{mOCS}/C_{aOCS} (0.0, 0.2) and g_{sOCS}/g_{iOCS} (0.1, 0.5) provide indication of the sensitivity of LRU to these variables and show a similar range, and nonlinear response, of LRU across a wide C_{iCO2}/C_{aCO2} range (Figure 1). It is assumed that biochemical demand for OCS is always high relative to supply due to the high affinity of CA for OCS [*Protoschill-Krebs et al.*, 1996]. When C_{iCO2}/C_{aCO2} is low, biochemical demand for CO_2 is high relative to supply. In this case, stomatal conductance largely controls fluxes, and relative fluxes are near 1.0 as a result, because C_{mOCS}/C_{aOCS} and C_{iCO2}/C_{aCO2} are similar in magnitude and stomatal conductances to OCS and CO_2 are similar in magnitude ($R_{CO2\text{-}OCS} = 1.2$; from *Seibt et al.* [2010]). When C_{iCO2}/C_{aCO2} is high, biochemical demand for CO_2 is low relative to supply. As a result, biochemical demand largely controls fluxes and relative fluxes are greater than 1.0, because C_{mOCS}/C_{aOCS} is much lower than C_{iCO2}/C_{aCO2}, but stomatal conductances to OCS and CO_2 remain similar in magnitude. The LRU range estimated from equation (6) (Figure 1) is close to the 1.4–3.4 range measured by *Sandoval-Soto et al.* [2005] for multiple species. *Seibt et al.* [2010] reported published values of LRU to range from 1.5–4.0, and derived a global mean LRU estimate of 2.8 ± 0.3. *Stimler et al.* [2010a] found LRU to be variable, dependent on environmental conditions, but found the range for three C_3 species to be approximately 1.0–4.0, similar that reported by *Seibt et al.* [2010]. The relationship between LRU and C_{iCO2}/C_{aCO2} in equation (6) provides means to estimate LRU in equations (1) and (5), but a limitation of these equations may be the LRU term, which would benefit from better characterization in future work.

3. Materials and Methods

[16] A study at the Harvard Forest AmeriFlux site (Table 1) was conducted to explore the utility of OCS measurements to estimate GPP. Following analysis at Harvard Forest, the potential magnitude of OCS signals were evaluated at five other AmeriFlux sites (Table 1) using OCS projections from CO_2 measurements, as OCS measurements were only available at Harvard Forest.

3.1. Flux Tower Observations: General

[17] For all sites, NEE, GPP, and friction velocity data were obtained from the Level 4 data archived on the AmeriFlux website (http://public.ornl.gov/ameriflux/). Level 4 flux data

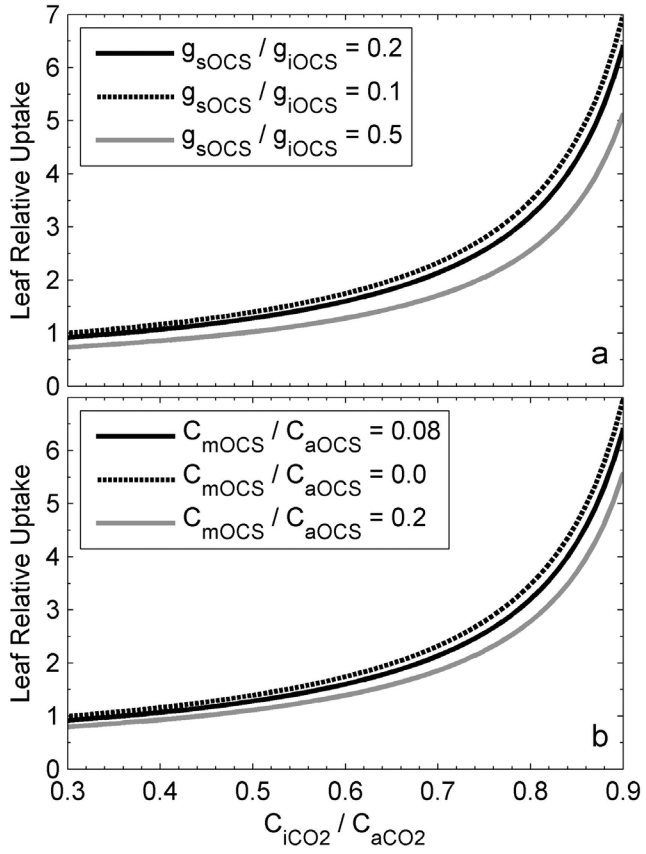

Figure 1. (a) LRU (leaf level OCS flux normalized by OCS mole fraction, divided by leaf level CO_2 flux normalized by CO_2 mole fraction) calculated from equation (6), and plotted versus intercellular to ambient CO_2 mole fraction ratio (C_{iCO2}/C_{aCO2}) for three different OCS stomatal to internal conductance ratios (g_{sOCS}/g_{iOCS}). (b) Same as Figure 1a except for three different mesophyll to ambient OCS mole fraction ratios (C_{mOCS}/C_{aOCS}). The values of g_{sOCS}/g_{iOCS} = 0.2 and C_{mOCS}/C_{aOCS} = 0.08 were taken from *Stimler et al.* [2010a] and are assumed representative of C_3 vegetation; the other g_{sOCS}/g_{iOCS} (0.1, 0.5) and C_{mOCS}/C_{aOCS} (0.0, 0.2) values show how the relationship between LRU and C_{iCO2}/C_{aCO2} changes when g_{sOCS}/g_{iOCS} and C_{mOCS}/C_{aOCS} vary.

provide measured (with standard eddy covariance techniques) and gap-filled NEE and friction velocity, and estimated GPP (level 4 products contain two GPP estimates; we used those derived from the method of *Reichstein et al.* [2005], where TER estimates derived from a nocturnal NEE versus temperature relationship, which includes nighttime temperature coefficients that are allowed to vary by season, are extrapolated to daytime and used to calculate GPP from NEE measurements, GPP = NEE – TER; hereafter these GPP estimates will be denoted GPP_{TER}). Vertical CO_2 mole fraction profile data were obtained from the AmeriFlux repository or directly from site investigators. CO_2 measurements at all sites were made with in situ infrared gas analyzers with associated uncertainty that differed among sites, but is estimated to be in the range of 0.2–1.0 μmol mol^{-1}. Measured and estimated data (NEE, GPP_{TER}, friction velocity, CO_2 mole fraction) are reported herein as the mean of eight

Table 1. Characteristics of AmeriFlux Sites Evaluated in This Study

Site	Latitude (°N)	Longitude (°W)	Elevation (m)	Vegetation Type	Flux (Above-Canopy) Measurement Height (m)	Canopy Height (m)	Within-Canopy CO_2 Measurement Height[a] (m)	Leaf Area Index (m^2 m^{-2})	Reference
Harvard Forest[b]	42.54	72.17	340	Mixed forest	29.0	23.0	18.3	5.5	*Urbanski et al.* [2007]
Morgan Monroe	39.32	86.41	275	Deciduous broadleaf forest	46.0	27.0	16.0	4.9	*Schmid et al.* [2000]
Willow Creek	45.81	90.08	515	Deciduous broadleaf forest	29.6	24.2	21.3	5.4	*Cook et al.* [2004]
Niwot Ridge	40.03	105.55	3050	Evergreen needleleaf forest	21.5	11.5	9.0	4.2	*Monson et al.* [2002]
Kendall Grassland	31.74	109.94	1530	C_4 grassland	6.4	0.5	0.5	1.0	*Scott et al.* [2010]
Rosemount Soybean	44.71	93.09	260	Soybean cropland	2.0	0.9	1.1	7.5	*Griffis et al.* [2005]

[a]Height at which the CO_2 difference from the above-canopy CO_2 measurement was calculated; the above-canopy CO_2 measurement height was at or near the flux measurement height for all sites except Morgan Monroe, where the above-canopy CO_2 measurement height was 32.0 m. Note that the within-canopy CO_2 measurement height is not actually within the canopy at the Rosemount Soybean site; there were no within-canopy CO_2 measurements at this site, thus 1.1 m was selected.
[b]Only site where OCS measurements were made, at 29.0 and 2.0 m (within canopy).

midday half hourly measurements centered on local noon unless otherwise indicated; negative NEE and GPP indicate uptake by the ecosystem.

3.2. Harvard Forest: OCS Mole Fraction Measurements

[18] Air samples were collected on the flux tower above (29.0 m) and within (2.0 m) the forest canopy within 2 h of each other in paired electropolished stainless steel flasks (2.5–3.0 l). Flask air samples were analyzed within approximately two weeks of sample collection, for OCS mole fraction with the National Oceanic and Atmospheric Administration's coupled gas chromatograph (GC)-mass spectrometer (MS) system as described in *Montzka et al.* [2004]. Median replicate injection precision for OCS mole fraction measurement at ambient levels during 2000–2006 was 0.4% (approximately 3000 samples), and 95% of the time it was less than 1.3% [*Montzka et al.*, 2007]. For each above- or within-canopy air sample collected, paired flasks were filled over 5–10 min, typically within 3 h of local noon. Above-canopy samples were collected approximately once every two weeks throughout the year in 2005 and 2006, providing a total of 70 above-canopy OCS mole fraction measurements. In 2005, 10 sets of above- and within-canopy samples were collected approximately once per week during the spring; sample collection began on day of year (DOY) 111 (21 April), before bud break, and ended on DOY 166 (15 June), after leaf expansion was complete. In 2006, 14 sets of above- and within-canopy samples were collected approximately once per week during the growing season; sample collection began on DOY 160 (9 June), after leaf expansion was complete, and ended on DOY 296 (23 October), near the time leaves fell. In 2006, two more sets of above- and within-canopy samples were collected after the growing season. In previous studies [*Montzka et al.*, 2004; 2007], OCS measurements were discarded when paired samples disagreed by more than 1.3% (approximately 6.3 pmol mol^{-1}). Only nine of the 96 total OCS mole fraction measurements from the paired flask samples collected were outside of this rejection threshold, with the highest paired sample difference being 12.5 pmol mol^{-1} (2.6%) and only one other being greater than 8.1 pmol mol^{-1} (1.7%). We retained these nine measurements in order to maximize the amount of data for analysis.

3.3. Harvard Forest: CO_2 Mole Fraction and CO_2 Flux Measurements

[19] CO_2 mole fractions at eight heights (ranging from 0.3 to 29.0 m) in the forest were determined by sequentially sampling each height through a series of solenoid valves mounted on the flux tower. Sample pressure was held constant (66.7 kPa) by modulating the flow to a bypass pump using a pressure controller (MKS, model 250B). A subsample was drawn through a Nafion dryer and −20°C cold trap into a CO_2 analyzer (LI-COR, model 6251), configured for differential measurement using a reference gas at near ambient CO_2 (approximately 380 μmol mol^{-1}). Pressure in the analyzer cell was maintained constant (64.0 kPa) using a second pressure controller. The CO_2 analyzer was calibrated approximately every 4 h with two working standards that spanned the typical range of ambient mole fractions. The working standards were calibrated to within 0.1 μmol mol^{-1} or better in the laboratory before and after use against a set of World Meteorological Organization primary standards (NOAA-GMD; http://www.esrl.noaa.gov/gmd/ccl/index.html). Ambient mole fractions were computed from a linear fit through the two calibration standards.

[20] CO_2 fluxes were determined by eddy covariance using a second CO_2 analyzer (LI-COR, model 6262), configured for fast response. The instrumental gain for the fast response analyzer was determined by standard addition calibration using a small volume of 1% CO_2 in air mixed into the sample flow [*Goulden et al.*, 1996] and cross-checked by regressing the fast response analyzer signal against the observed profile mole fraction for the time intervals when the two analyzers were sampling from the same height.

3.4. Harvard Forest: CO_2 and OCS Gradients and Ecosystem Relative Uptake (ERU)

[21] CO_2 gradients were calculated by taking the difference between CO_2 mole fractions at 18.3 m (top of canopy is approximately 23.0 m) and 29.0 m (flux measurement height) and dividing by the measurement height difference. The 18.3 m measurement height was used for CO_2 gradient calculation because CO_2 drawdown was maximal at this within-canopy height; at lower heights CO_2 mole fractions were highly influenced by soil respiration (Figure 2a). Ideally, CO_2 and OCS mole fraction gradients should be calculated with measurements from colocated sampling heights, but OCS mole fractions were only measured at 2.0 and 29.0 m. OCS gradients were calculated with two methods. First, a linear OCS gradient between 29.0 and 2.0 m was assumed and gradients were calculated by taking the difference between OCS mole fractions at 2.0 and 29.0 m and dividing by the measurement height difference. Second, it was assumed that the shape of OCS profile was similar to the concurrently measured ozone (O_3) profile (Figures 2b and 2c); OCS mole fractions were approximated for 18.3 m (colocated with the within-canopy CO_2 mole fraction measurement) from the shape of the O_3 profiles. Plant canopies are an O_3 sink through leaf O_3 uptake, surface O_3 deposition, and O_3 reactions with plant-produced volatile organic compounds (VOCs) within the canopy air space. Some studies have shown that O_3 reaction with VOCs dominate over leaf O_3 uptake through stomata [*Goldstein et al.*, 2004; *Kurpius and Goldstein*, 2003], whereas others have found a larger dominance of stomatal O_3 uptake [*Munger et al.*, 1996; *Turnipseed et al.*, 2009]. Thus, the O_3 profile is not an excellent OCS profile analog. However, leaf O_3 uptake, surface O_3 deposition, and O_3 reactions with VOCs are all within-canopy processes, as is leaf OCS uptake through stomata. Given that OCS data were only available at two heights, 2.0 and 29.0 m, both methods to derive OCS gradients were used in subsequent calculations and results were compared. OCS profiles and gradients will be referred to as either linear or O_3 shaped. The OCS mole fraction at 18.3 m (OCS_{18m}) was estimated from measured OCS mole fractions at 29.0 and 2.0 m (OCS_{29m} and OCS_{2m}, respectively) and O_3 mole fractions at 29.0, 18.3, and 2.0 m (O_{3-29m}, O_{3-18m}, and O_{3-2m}, respectively; O_{3-2m} was calculated by linearly interpolating the O_3 mole fraction measurements at 4.5 and 0.8 m)

$$OCS_{18m} = OCS_{29m} - (OCS_{29m} - OCS_{2m})\left(\frac{O_{3-29m} - O_{3-18m}}{O_{3-29m} - O_{3-2m}}\right) \quad (7)$$

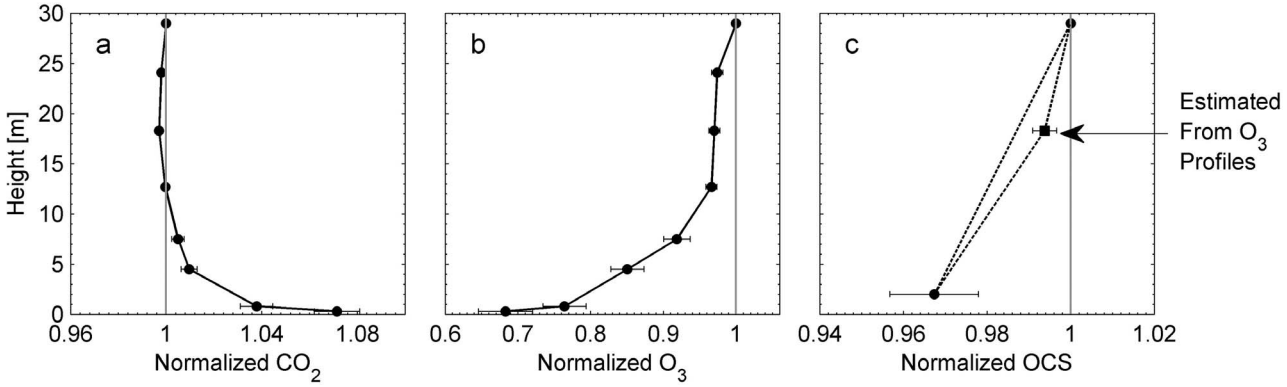

Figure 2. Harvard Forest mean normalized (a) CO_2, (b) O_3, and (c) OCS mole fraction profiles calculated from the 12 days during the 2006 growing season when OCS measurements were made. Normalized mole fractions were calculated by dividing the mole fraction at each height by the mole fraction at 29.0 m; error bars show standard deviation of the mean at each height (in some cases error bars are smaller than symbols). Two OCS profiles are shown: linear profile between 29.0 and 2.0 m (the only two heights at which OCS mole fractions were measured) and an OCS profile with an estimated datum at 18.3 m (square symbol in Figure 2c), which was based on the shape of the O_3 profiles measured at the time of air sample collection for OCS analysis and calculated from equation (7). OCS data were typically collected within 3 h of local noon and within- and above-canopy measurements were typically made within less than 2 h of each other; CO_2 and O_3 data are mean values calculated from half hourly means corresponding to the time of OCS measurements.

where OCS mole fractions are (pmol mol^{-1}) and O_3 mole fractions are (nmol mol^{-1}). O_3 mole fractions were measured at the same heights as CO_2 mole fractions by sequentially sampling through the same series of solenoid valves mounted on the flux tower [*Horii et al.*, 2004; *Munger et al.*, 1998]. A subsample was drawn directly from the sample manifold into a UV absorbance O_3 analyzer (Dasibi 1008, model TEI49c). Calibration of the O_3 analyzer was checked periodically by supplying known O_3 mole fractions from a factory calibrated O_3 generator/analyzer.

[22] Measured CO_2 gradients and OCS gradients (from the linear OCS profiles) were linearly regressed against NEE and GPP_{TER}, respectively, to evaluate the influence of vegetation uptake on gradients (OCS gradients were not used to directly estimate OCS uptake or GPP, only to partition measured NEE as described in section 3.5). CO_2 gradients were analyzed relative to NEE because CO_2 is both assimilated and released by the forest. OCS gradients were analyzed relative to GPP_{TER} because OCS is presumably taken up by the forest, but not released. CO_2 and OCS gradients were also linearly regressed against friction velocity to evaluate the influence of turbulence and atmospheric mixing. CO_2 mole fraction, NEE, GPP_{TER}, and friction velocity were calculated by averaging mean half hourly values over the time period of the within- and above-canopy OCS measurements (typically a 2 h or shorter time period). In addition to analysis of OCS gradients calculated from OCS mole fraction measurements, anticipated OCS gradients were estimated from measured CO_2 gradients and regressed against GPP_{TER} and friction velocity. These anticipated OCS gradients, estimated from only CO_2 gradients, are hereafter referred to as projected OCS gradients and were calculated with equations (2)–(4), assuming colocated measurement heights for OCS and CO_2, an ERU of 4, and an above-canopy OCS mole fraction of 400 pmol mol^{-1} (these assumptions produce projected OCS gradients for the same time frame and height difference as the CO_2 gradients). Projected OCS gradients allow a comparison to the measured OCS gradients at Harvard Forest and to projected OCS gradients from the other AmeriFlux sites (described in section 3.7).

[23] Two calculations of ERU were made. First, ERU was calculated with equations (2)–(4) from time periods when simultaneous within- and above-canopy OCS and CO_2 measurements were available; this yielded nine individual ERU values (one from 2005 and eight from 2006) representative of midday conditions when the measurements were made; hereafter these ERU values will be referred to as short-term ERU. Short-term ERU could not be calculated on 5 days (1 day from 2005 and 4 days from 2006) because either the CO_2 or OCS gradient, or both, were positive, indicating strong vertical mixing or less uptake compared to other days. Second, ERU was calculated as the slope of the line between a plot of the 12 corresponding relative OCS gradients and relative CO_2 gradients from the 2006 growing season; this method yielded a single ERU value representative of the 2006 growing season and hereafter will be referred to growing season ERU. Though a total of 26 paired flask samplings (above and within canopy) were obtained during 2005 and 2006, in 2005 only two sets and in 2006 only 12 sets of above- and within-canopy samples were available for ERU calculation because corresponding CO_2 mole fraction measurements were only available for these subsets of the OCS data.

3.5. Harvard Forest: Comparison of GPP Estimates and Uncertainties

[24] Estimates of GPP from OCS-based NEE partitioning, hereafter denoted GPP_{OCS}, were calculated from equation (5) using short-term and growing season ERU and NEE measurements from the flux tower. This requires a value for LRU

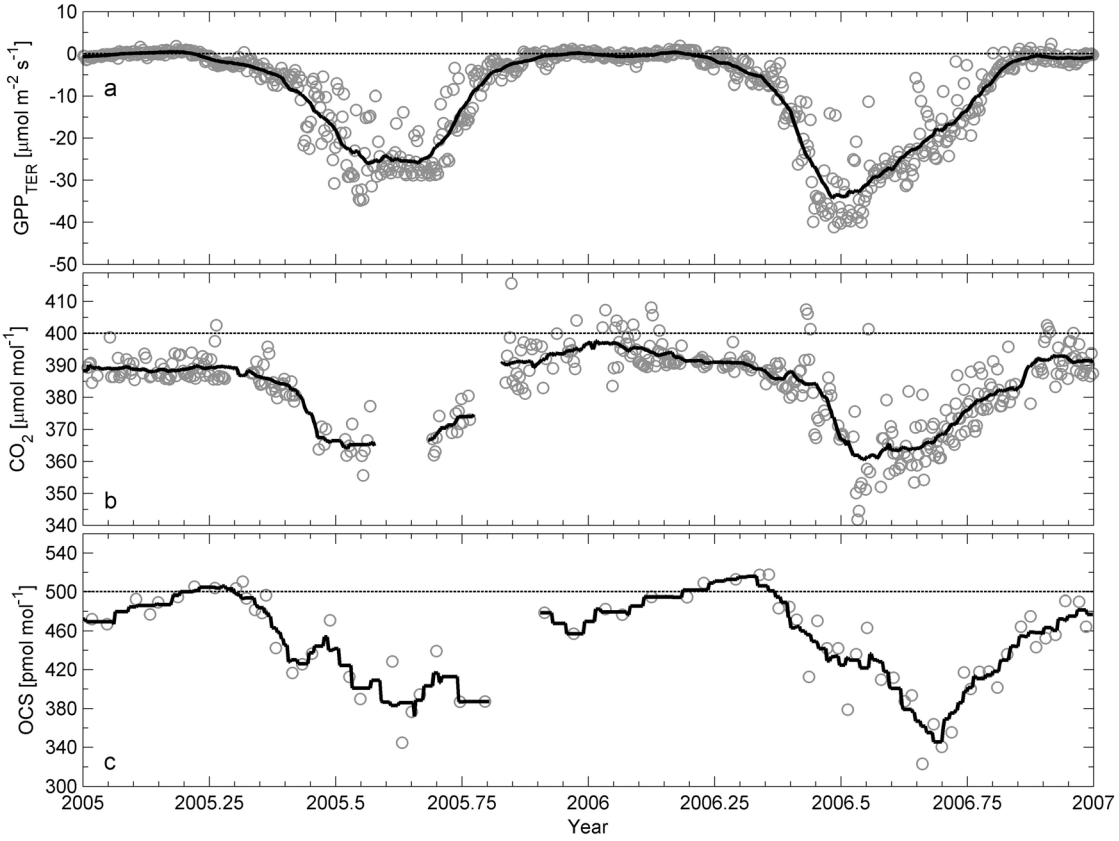

Figure 3. (a) Harvard Forest gross primary production estimates from net ecosystem exchange partitioning via the method of *Reichstein et al.* [2005] (GPP_{TER}), (b) CO_2 mole fraction measurements at 29.0 m, and (c) OCS mole fraction measurements at 29.0 m. GPP_{TER} and CO_2 data are mean values calculated from eight half hourly means centered on local noon; OCS data are from air samples typically collected within 3 h of local noon. Solid lines are 31 day means centered on each day of year.

in equation (5), which was estimated from equation (6) by assuming $C_{iCO2}/C_{aCO2} = 0.79$ (value given by *Seibt et al.* [2010] for cool deciduous forests) and $g_{sOCS}/g_{iOCS} = 0.20$ and $C_{mOCS}/C_{aOCS} = 0.08$ (approximate values given by *Stimler et al.* [2010a] for C_3 species), yielding LRU = 3.0, which is within the uncertainty of the global mean LRU estimate, 2.8 ± 0.3, reported by *Seibt et al.* [2010]. GPP_{OCS} estimates were then compared to GPP_{TER} estimates for the time periods coincident with ERU values. GPP_{TER} uncertainty was assumed to be 20%, based on calculations that accounted for choice of partitioning algorithm and data gaps [*Desai et al.*, 2008]. GPP_{OCS} uncertainty was calculated by propagating the uncertainties of NEE, ERU, and LRU through the calculation of GPP_{OCS} from equation (5) using standard error propagation techniques [*Taylor*, 1997]. Uncertainty for the NEE measurements at Harvard Forest was assumed to be 2.3 μmol m^{-2} s^{-1} [*Richardson et al.*, 2006]. Uncertainty for ERU was calculated from the CO_2 and OCS gradient measurements for short-term ERU (O_3 gradient measurements were included in the ERU uncertainty calculation from the O_3-shaped OCS profiles), and was calculated as the standard error of the slope of the line between the plot of relative OCS gradients and relative CO_2 gradients for growing season ERU. Measurements of LRU were not made, but *Seibt et al.* [2010] and *Stimler et al.* [2010a] reported approximate ranges of 1.5–4.0 and 1.0–4.0, respectively. The approximated LRU of 3 for Harvard Forest lies within these ranges and an arbitrary uncertainty of 1.5 (approximately half the reported LRU ranges) was assigned because 3 ± 1.5 approximates these ranges.

3.6. Harvard Forest: Estimation of OCS Flux Magnitude and Above-Canopy OCS Gradients

[25] Fluxes of OCS for 2006 were estimated from equation (1) using GPP_{TER}, above-canopy CO_2 and OCS mole fraction measurements, and an LRU of 3 (again, calculated from equation (6) assuming $C_{iCO2}/C_{aCO2} = 0.79$, $g_{sOCS}/g_{iOCS} = 0.20$, and $C_{mOCS}/C_{aOCS} = 0.08$). This provided estimates of the GPP-driven OCS flux at Harvard Forest for comparison with previous studies where canopy-scale OCS flux was measured. Above-canopy OCS mole fraction gradients ($\partial OCS/\partial z$) were estimated from the OCS flux estimates via Monin-Obukhov Similarity Theory (MOST), assuming neutral conditions [*Wyngaard*, 2010]

$$\frac{\partial \mathrm{OCS}}{\partial z} = \frac{\mathrm{OCS}*}{kz} \tag{8}$$

where OCS_* is OCS flux divided by friction velocity, k is the von Kármán constant (assumed to be 0.4), and z is height above the surface (29.0 m; flux measurement height). In order to produce OCS gradients in units of (pmol mol^{-1} m^{-1}),

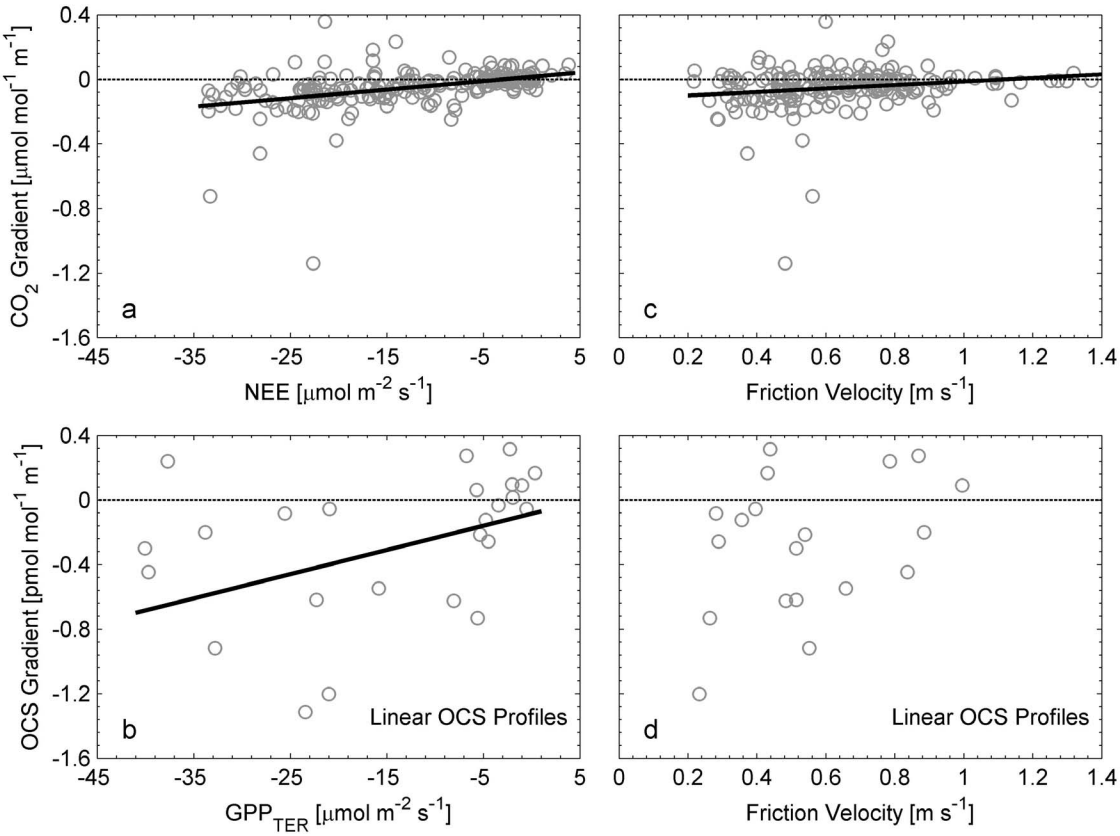

Figure 4. Harvard Forest CO_2 gradients (CO_2 at 18.3 m minus CO_2 at 29.0 m, divided by the height difference) versus (a) NEE ($y = 0.0053x + 0.015$, $r^2 = 0.16$, slope $P < 0.001$, intercept is not significant) and (c) friction velocity ($y = 0.11x - 0.12$, $r^2 = 0.04$, slope $P < 0.025$, intercept $P < 0.001$). Harvard Forest OCS gradients, assuming a linear OCS profile (OCS at 2.0 m minus OCS at 29.0 m, divided by the height difference), versus (b) gross primary production estimates from NEE partitioning via the method of *Reichstein et al.* [2005] (GPP_{TER}) ($y = 0.015x - 0.085$, $r^2 = 0.17$, slope $P < 0.05$, intercept is not significant) and (d) friction velocity ($y = 0.66x - 0.70$, $r^2 = 0.09$, slope is not significant, intercept $P < 0.05$). OCS data were typically collected within 3 h of local noon and within- and above-canopy measurements were typically made within less than 2 h of each other; CO_2, NEE, GPP_{TER}, and friction velocity data points are mean values calculated from half hourly means corresponding to the time of OCS measurements.

$\partial OCS/\partial z$ from equation (8) was divided by the molar density of air (mol m^{-3}) calculated from measured air temperature. This provided estimates of the GPP-driven surface layer OCS gradients over the canopy at Harvard Forest, which are useful to estimate analytical requirements for future studies.

3.7. Projection of OCS Gradients at Additional AmeriFlux Sites

[26] Calculation of projected OCS gradients at other flux tower sites allowed comparison to Harvard Forest and evaluation of the potential magnitude of OCS signals at sites where OCS measurements have not yet been made. Measured CO_2 gradients and projected OCS gradients were calculated as described for Harvard Forest at five other AmeriFlux sites (Table 1). To project OCS gradients at Kendall Grassland, a warm season C_4 grassland, we assumed an ERU of 4, as with the C_3 ecosystems. However, little work on OCS uptake has been done on C_4 leaves and in C_4 ecosystems. The assumption that C_4 ecosystems are similar to C_3 ecosystems is based on results from *Sandoval-Soto et al.* [2005], who found similar relative uptake ratios for corn leaves and C_3 leaves reported in the literature. We note, however, that CA activity is much lower in C_4 plants [*Gillon and Yakir*, 2000], and this may mean our assumed ERU at Kendall Grassland was inappropriate. As with Harvard Forest, measured CO_2 gradients and projected OCS gradients were linearly regressed against NEE and GPP_{TER}, respectively, and friction velocity, to evaluate the influence of vegetation uptake and atmospheric mixing on measured gradients for CO_2 and anticipated gradients for OCS.

4. Results

4.1. Harvard Forest

[27] GPP_{TER} and above-canopy CO_2 and OCS mole fractions followed similar seasonal patterns in 2005 and 2006 at Harvard Forest (Figure 3). The highest photosynthetic uptake rates (most negative GPP_{TER}) were near -40 μmol m^{-2} s^{-1} in early summer, approximately halfway through the year. Seasonal decreases in CO_2 and OCS mole fractions above the canopy in spring were coincident with photosynthetic uptake, but minimum CO_2 lagged behind maximum GPP_{TER} in 2006,

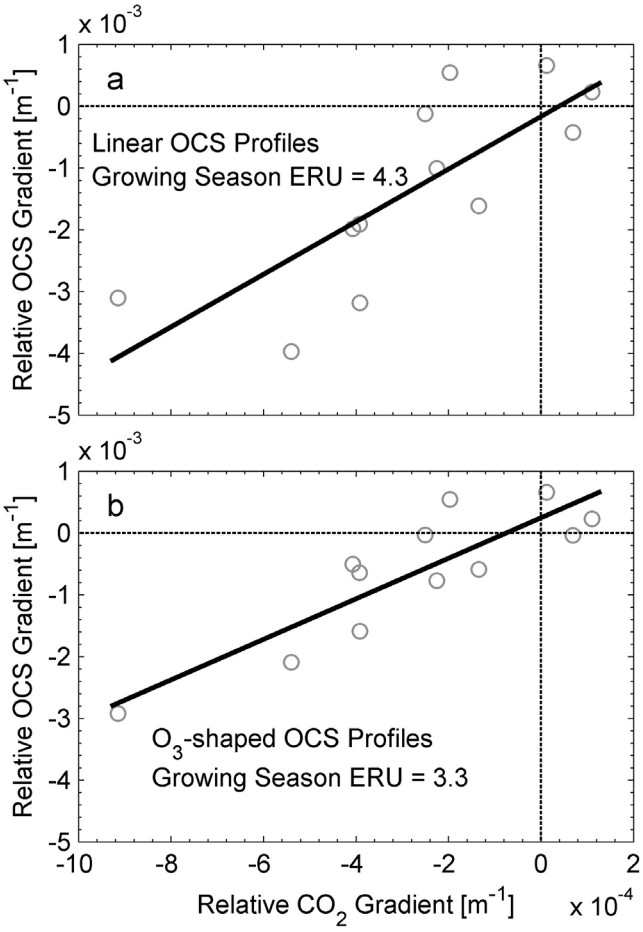

Figure 5. Harvard Forest relative OCS gradients (calculated from equation (2)) versus relative CO_2 gradients (calculated from equation (3)). CO_2 gradients were directly calculated from mole fraction measurements at 29.0 m and 18.3 m. OCS gradients were calculated for the 29.0 m and 18.3 m height difference using mole fraction measurements at 29.0 m and 2.0 m and (a) assuming a linear profile between 29.0 m and 2.0 m ($y = 4.26x - 0.00$, $r^2 = 0.61$, slope $P < 0.01$, intercept is not significant) and (b) estimating the OCS mole fraction at 18.3 m based on the shape of the O_3 profiles measured at the time of air sample collection for OCS analysis (equation (7); see section 3.4 for details) ($y = 3.28x + 0.00$; $r^2 = 0.76$; slope $P < 0.001$, intercept is not significant). Data are from the 2006 growing season only, and slopes of the lines are representative of ERU over the time period when the data were collected, days of year 160–296. OCS data were typically collected within 3 h of local noon and within- and above-canopy measurements were typically made within less than 2 h of each other; CO_2 data are mean values calculated from half hourly means corresponding to the time period of OCS measurements.

and minimum OCS lagged behind minimum CO_2 and even further behind maximum GPP_{TER}.

[28] CO_2 gradients were linearly correlated with NEE and showed a trend of more drawdown (more negative gradients) with increasing NEE (Figure 4a; $y = 0.0053x + 0.015$, $r^2 = 0.16$, slope $P < 0.001$, intercept is not significant). CO_2 gradients were also correlated with friction velocity and showed more drawdown at lower friction velocity (Figure 4c; $y = 0.11x - 0.12$, $r^2 = 0.04$, slope $P < 0.025$, intercept $P < 0.001$). OCS gradients were correlated with GPP_{TER} and showed a trend of more drawdown with increasing GPP_{TER} (Figure 4b; $y = 0.015x - 0.085$, $r^2 = 0.17$, slope $P < 0.05$, intercept is not significant), similar to the relationship between CO_2 gradients and NEE. The relationship between OCS gradients and friction velocity was not significant (Figure 4d; $y = 0.66x - 0.70$, $r^2 = 0.09$, slope is not significant, intercept $P < 0.05$).

[29] Relative OCS gradients were linearly correlated with relative CO_2 gradients, regardless of the method used to interpolate the available OCS data to derive gradients (Figure 5; data are from the 2006 growing season only). Regressions were similar for linear OCS profiles (Figure 5a; $y = 4.26x - 0.00$, $r^2 = 0.61$, slope $P < 0.01$, intercept is not significant) and O_3-shaped OCS profiles (Figure 5b; $y = 3.28x + 0.00$; $r^2 = 0.76$; slope $P < 0.001$; intercept is not significant). The slopes of the lines (4.3 ± 1.1 in Figure 5a and 3.3 ± 0.6 in Figure 5b) represent growing season ERU values for 2006. Short-term ERU values (ratio of the relative OCS gradient to the relative CO_2 gradient for each datum) from 2006 ranged from 0.5 to 12.0 with a mean of 5.7 ± 1.2 (standard deviation of the mean) for ERU from linear OCS profiles and 0.1–4.4 with a mean of 2.8 ± 0.5 (standard deviation of the mean) for ERU from O_3-shaped OCS profiles. Data on DOY 166, 173, 272, and 296 were not included in the calculation of mean short-term ERU because CO_2 and/or OCS gradients were positive and near zero, indicating strong vertical mixing, near balance between uptake and release, or no uptake. NEE and GPP_{TER} on DOY 166 and 173 were near -30 μmol m^{-2} s^{-1} and comparable to other days during the middle of the growing season, however, friction velocity was also higher on these days (0.88 and 0.79 m s^{-1}, respectively) compared to other days during the middle of the growing season (friction velocity was typically less than 0.6 m s^{-1}). On DOY 272 and 296, near the end of the growing season, NEE and GPP_{TER} were low, less than -7 μmol m^{-2} s^{-1}, compared to other days during the middle growing season, and friction velocity was also high (0.87 and 1.00 m s^{-1}, respectively). Vertical mixing and/or near zero uptake may have contributed to the near zero and/or positive gradients on DOY 166, 173, 272, and 296.

[30] Estimates of GPP_{OCS} calculated from NEE and short-term ERU (data from Figure 5) in equation (5), assuming LRU = 3 (calculated from equation (6)), were relatively consistent with the 1:1 line and correlated to GPP_{TER} (Figures 6a and 6b; $y = 1.26x - 4.31$; $r^2 = 0.77$, $P < 0.1$ (slope), standard error of slope = 0.62 for ERU from linear OCS profiles; $y = 0.82x + 2.30$; $r^2 = 0.44$, $P < 0.05$ (slope), standard error of slope = 0.35 for ERU from O_3-shaped OCS profiles). Estimates of GPP_{OCS} calculated from NEE and growing season ERU (constant ERU = 4.3 from linear OCS profiles and ERU = 3.3 from O_3-shaped OCS profiles) in equation (5) were similar in magnitude to GPP_{TER} (Figure 6c; $y = 1.28x + 3.11$, $r^2 = 0.99$, slope $P < 0.001$, standard error of slope = 0.01 for ERU = 4.3; $y = 0.99x + 2.39$, $r^2 = 0.99$, slope $P < 0.001$, standard error of slope = 0.01 for ERU = 3.3). It is important to note, however, when growing season ERU is used to estimate GPP_{OCS} (Figure 6c), variability originates from variability in NEE, just as variability in GPP_{TER} originates from variability in NEE. Thus, the high correlation (Figure 6c) is driven by NEE variability, as growing season

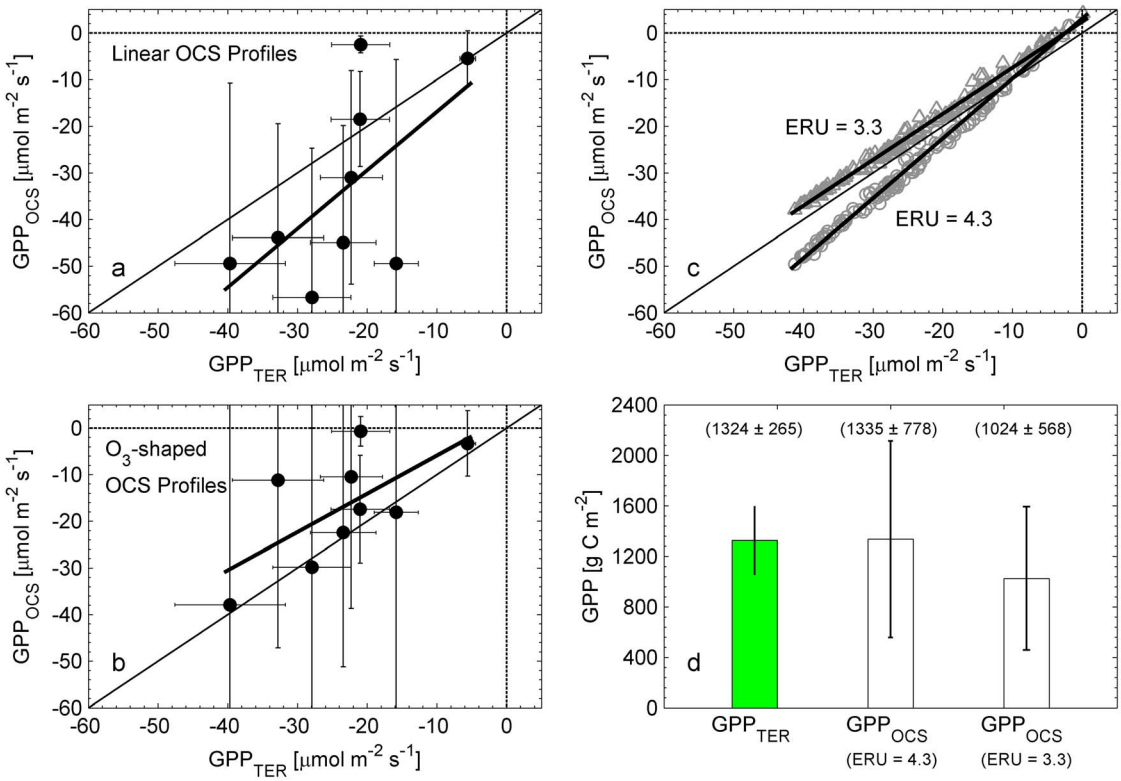

Figure 6. Harvard Forest gross primary production estimates from net ecosystem exchange partitioning via the method of *Reichstein et al.* [2005] (GPP_{TER}) and equation (5) (GPP_{OCS}). GPP_{OCS} was calculated for 9 different days based on the short-term ERU estimate for each day; ERU was estimated from the (a) linear OCS profile ($y = 1.26x - 4.31$, $r^2 = 0.37$, $P < 0.1$) and (b) O_3-shaped OCS profile ($y = 0.82x + 2.30$, $r^2 = 0.44$, $P < 0.05$). GPP_{OCS} was derived from NEE scaled by the growing season ERU values taken from the slopes of the lines in Figure 5 (ERU from linear OCS profiles is 4.3 and ERU from O_3-shaped OCS profiles is 3.3). OCS measurements spanned day of year 160–296 in 2006; (c) mean midday GPP for all days ($y = 1.28x + 3.11$, $r^2 = 0.99$, slope $P < 0.001$, standard error of slope = 0.01 for ERU = 4.3 and $y = 0.99x + 2.39$, $r^2 = 0.99$, slope $P < 0.001$, standard error of slope = 0.01 for ERU = 3.3) and (d) sum of GPP during daylight hours for all days. In Figures 6a–6d, LRU (in equation (5)) was estimated as 3 (calculated from equation (6)). OCS data were typically collected within 3 h of local noon and within- and above-canopy measurements were typically made within less than 2 h of each other; GPP_{TER} data are mean values calculated from half hourly means corresponding to the time period of OCS measurements.

ERU represents a constant scaling factor, along with LRU, used in equation (5) to partition NEE. On average, when using growing season ERU, GPP_{OCS} estimates were greater than GPP_{TER} by 3.6 μmol m^{-2} s^{-1} with a standard deviation of 3.2 μmol m^{-2} s^{-1} for ERU = 4.3, and less than GPP_{TER} estimates by 2.7 μmol m^{-2} s^{-1} with a standard deviation of 0.9 μmol m^{-2} s^{-1} for ERU = 3.3. When GPP was summed over DOY 160–296, for all daylight hours, GPP_{OCS} calculated with ERU = 4.3 was 1% higher than GPP_{TER}, and GPP_{OCS} calculated with ERU = 3.3 was 23% lower than GPP_{TER} (Figure 6d).

[31] Estimated OCS fluxes from equation (1), using GPP_{TER} estimates and assuming LRU = 3 (calculated from equation (6)), ranged from approximately 0 to −140 pmol m^{-2} s^{-1} (negative sign indicates assimilation) during 2006 (Figure 7a), with a range of approximately −10 to −140 pmol m^{-2} s^{-1} when leaves were present on trees. Estimated above-canopy (surface layer) OCS gradients from equation (8), assuming OCS flux estimates were representative of GPP-driven flux, ranged from approximately 0 to −0.6 pmol mol^{-1} m^{-1} (negative sign indicates drawdown) during 2006 (Figure 7b).

4.2. Anticipated OCS Gradients at the Additional Sites

[32] Measured CO_2 gradients and projected OCS gradients were linearly correlated with NEE and GPP_{TER}, respectively, at the five other AmeriFlux sites (Table 2 and Figure 8; measurements and projections at Harvard Forest are included for comparison). Measured CO_2 gradients and projected OCS gradients were also correlated with friction velocity at all sites (data not shown). Data from two broadleaf deciduous forests (Morgan Monroe State Forest and Willow Creek), with similar canopy structure and GPP_{TER} seasonality and magnitude as Harvard Forest, showed similar CO_2 gradients and as a result similar projected OCS gradients, compared to each other and Harvard Forest. Data from a subalpine conifer forest (Niwot Ridge) showed lower GPP_{TER} relative to the other forest sites, but similar CO_2 gradients and projected OCS gradients. Data from a warm season C_4 grassland (Kendall Grassland) and a C_3 agricultural ecosystem

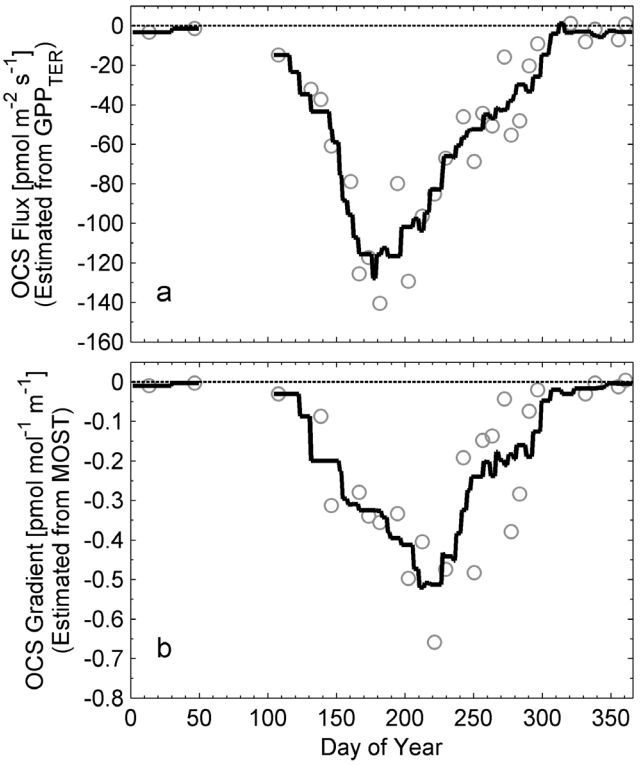

Figure 7. Harvard Forest (a) OCS fluxes estimated from gross primary production estimates from net ecosystem exchange partitioning via the method of *Reichstein et al.* [2005] (GPP_{TER}) and (b) above-canopy (surface layer) OCS gradients estimated from MOST for 2006. OCS flux estimates were calculated from equation (1) using only above-canopy CO_2 and OCS mole fraction measurements and GPP_{TER}. Leaf relative uptake (LRU in equation (1)) was estimated as 3 (calculated from equation (6)). OCS gradient estimates were calculated from equation (8) using the OCS flux estimates from Figure 7a and friction velocity measurements at 29.0 m (flux measurement height). GPP_{TER} and CO_2 data used to estimate OCS fluxes and friction velocity data used to estimate OCS gradients were mean values calculated from eight half hourly means centered on local noon; OCS data used in the estimate were from air samples typically collected within 3 h of local noon. The solid line is a 31 day mean centered on each day of year. Only data from 2006 are shown because simultaneous above-canopy CO_2 and OCS measurements were unavailable due to missing CO_2 data on many of the days in 2005.

(Rosemount Soybean) showed much larger CO_2 gradients for similar NEE relative to the forests, and therefore, much larger projected OCS gradients for similar GPP_{TER} relative to the forests.

[33] Measured CO_2 gradients and projected OCS gradients were summarized for all sites for comparison (Table 3). Gradients for the deciduous forests (Harvard Forest, Morgan Monroe State Forest, and Willow Creek) and the subalpine conifer forest (Niwot Ridge) were similar. Gradients for the warm season C_4 grassland (Kendall Grassland) and soybean crop (Rosemount Soybean) were approximately 4 and 20 times greater than gradients at the forest site with the highest gradients (Willow Creek), respectively.

5. Discussion

5.1. Harvard Forest

[34] The seasonal patterns of above-canopy CO_2 and OCS mole fractions at Harvard Forest in 2005 and 2006 were closely related (Figure 3), as has been shown for previous years [*Montzka et al.*, 2007]. Seasonal dynamics of both gases were also related to the seasonal pattern of GPP_{TER} (Figure 3). The peak-to-peak seasonal change in the above-canopy OCS mole fraction was approximately 150 pmol mol^{-1}, compared to a peak-to-peak seasonal change of approximately 30 μmol mol^{-1} for the above-canopy CO_2 mole fraction. When the minimum summertime OCS mole fraction was referenced to a late winter/early spring OCS maximum of approximately 500 pmol mol^{-1} and the minimum CO_2 mole fraction was referenced to a late winter/early spring CO_2 maximum of approximately 390 μmol mol^{-1}, the relative regional net uptake of OCS was approximately 4 times that of CO_2. This is slightly lower than the mean hemispheric value derived by *Montzka et al.* [2007], who reported that the relative variation in the OCS mole fraction seasonal amplitude at multiple sites in the northern hemisphere (including Harvard Forest, and coastal and marine sites that may be influenced by factors beyond uptake by vegetation) during 2000–2005 averaged 6 ± 1 times larger than the relative variation in the CO_2 mole fraction seasonal amplitude. The summer minimum in CO_2 mole fraction represents the point in time where CO_2 uptake and emission are equal over the broad region influencing mole fractions measured at Harvard Forest. After the minimum, emission is presumably greater than uptake and CO_2 mole fraction increases. For the OCS mole fraction,

Table 2. Summary of Linear Regression Statistics for Measured CO_2 Mole Fraction Gradients Versus NEE and Projected OCS Mole Fraction Gradients Versus Gross Primary Production at All Sites Evaluated[a]

Site	Measured CO_2 Gradients[b] Versus NEE			Projected OCS Gradients[c] Versus GPP		
	Slope[d]	Intercept[e]	r^2	Slope[d]	Intercept[e]	r^2
Harvard Forest	0.0034	0.0021	0.12	0.014	0.052	0.12
Morgan Monroe	0.0030	−0.0038	0.20	0.011	−0.0052	0.17
Willow Creek	0.0068	−0.0024	0.32	0.027	0.076	0.32
Niwot Ridge	0.0083	0.0045	0.41	0.026	0.030	0.36
Kendall Grassland	0.072	−0.11	0.78	0.30	0.041	0.75
Rosemount Soybean	0.20	−0.27	0.61	0.76	1.69	0.65

[a] Site details are provided in Table 1.

[b] Calculated by taking the difference between within- and above-canopy CO_2 measurements, at the heights reported in Table 1, and dividing the CO_2 difference by the measurement height difference.

[c] Calculated from measured CO_2 gradients via equations (2)–(4), assuming colocated measurement heights for OCS and CO_2, ecosystem relative uptake (ERU) was 4, and above-canopy OCS mole fraction was 400 pmol mol^{-1} (assumptions produce projected OCS gradients for the same time frame and height difference as CO_2 gradients).

[d] All slopes were significantly different from zero at the $P < 0.001$ level; units are μmol mol^{-1} m^{-1}/μmol m^{-2} s^{-1} and pmol mol^{-1} m^{-1}/μmol m^{-2} s^{-1} for CO_2 and OCS, respectively.

[e] Units are μmol mol^{-1} m^{-1} and pmol mol^{-1} m^{-1} for CO_2 and OCS, respectively.

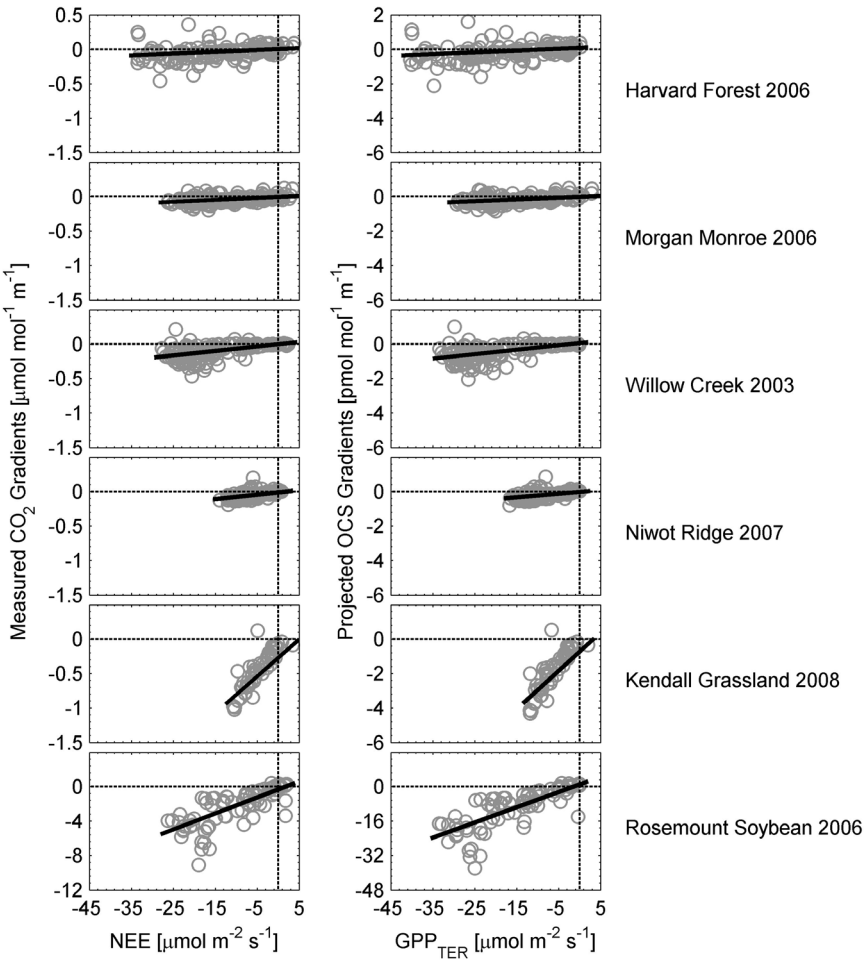

Figure 8. Relationship between measured CO_2 gradients (within-canopy minus above-canopy CO_2 mole fraction, divided by the difference between measurement heights) and (left) measured NEE and (right) projected OCS gradients and gross primary production estimates from NEE partitioning via the method of *Reichstein et al.* [2005] (GPP_{TER}), at all six AmeriFlux sites evaluated. Projected OCS gradients were calculated with equations (2)–(4), assuming colocated measurement heights for OCS and CO_2, an ecosystem relative uptake (ERU) of 4, and an above-canopy OCS mole fraction of 400 pmol mol^{-1} (assumptions produce projected OCS gradients for the same time frame and height difference as CO_2 gradients). All data are mean values calculated from eight half hourly means centered on local noon. Ameriflux site details are given in Table 1, statistics for the linear regressions are given in Table 2, and summary statistics for CO_2 and OCS gradients at each site are given in Table 3.

Table 3. Summary of Measured CO_2 Mole Fraction Gradients and Projected OCS Mole Fraction Gradients at All Sites Evaluated[a]

	Measured CO_2 Gradients[b] (μmol mol^{-1} m^{-1})				Projected OCS Gradients[c] (pmol mol^{-1} m^{-1})			
Site	Mean	SD	Minimum	Maximun	Mean	SD	Minimum	Maximun
Harvard Forest	−0.04	0.10	−0.46	0.36	−0.18	0.44	−2.13	1.61
Morgan Monroe	−0.04	0.05	−0.19	0.12	−0.18	0.20	−0.83	0.51
Willow Creek	−0.10	0.11	−0.46	0.22	−0.43	0.47	−2.05	1.02
Niwot Ridge	−0.05	0.05	−0.19	0.20	−0.20	0.19	−0.79	0.85
Kendall Grassland	−0.45	0.28	−1.02	0.13	−1.90	1.18	−4.31	0.54
Rosemount Soybean	−2.04	2.14	−9.08	0.38	−8.89	9.37	−37.82	1.56

[a]Site details are provided in Table 1. SD is standard deviation.
[b]Calculated by taking the difference between within- and above-canopy CO_2 measurements, at the heights reported in Table 1, and dividing the CO_2 difference by the measurement height difference.
[c]Calculated from measured CO_2 gradients via equations (2)–(4), assuming colocated measurement heights for OCS and CO_2, ERU was 4, and above-canopy OCS mole fraction was 400 pmol mol^{-1} (assumptions produce projected OCS gradients for the same time frame and height difference as CO_2 gradients).

the summer minimum was considerably later (approximately 6–8 weeks) than that for CO_2 (Figures 3b and 3c). This is likely due in part to a lack of OCS release analogous to respiratory release of CO_2, thus the OCS mole fraction decreases until OCS uptake no longer occurs. Increase at the point of measurement occurs due to transport of background air with higher mole fraction.

[35] At Harvard Forest, CO_2 gradients were correlated with NEE (Figure 4a) and OCS gradients were correlated with GPP_{TER} (Figure 4b), but strong relationships between gradients and fluxes are not necessarily expected because the magnitude of gradient for a given flux depends on intensity of vertical mixing. At higher friction velocity, mixing of within- and above-canopy air was enhanced and CO_2 and OCS gradients were diminished as expected, even when NEE and GPP_{TER} were high (Figures 4c and 4d). Thus, vertical mixing may have contributed to the near zero and/or positive gradients observed on some days (DOY 166 and 173 for OCS gradients), indicating the challenge of measuring ERU over short time periods. Previous studies have found larger OCS gradients under more stable conditions when mixing was reduced [*Mihalopoulos and Nguyen*, 2001; *White et al.*, 2010].

[36] Despite differing within-canopy measurement heights and measurement time frames for OCS mole fractions and CO_2 and OCS gradients, relative OCS and CO_2 gradients were linearly correlated during the 2006 growing season (Figure 5), suggesting the likelihood of similar mechanisms controlling their magnitude and dynamics during the daytime. Measured gradients were due in part to photosynthetic uptake, indicated by the relationships between gradients and CO_2 fluxes (Figures 4a and 4b). However, CO_2 gradients result from the balance between uptake and release, whereas OCS gradients are assumed to be affected by uptake only. Thus, relative uptake of OCS should be greater than that of CO_2. Our results were consistent with this perspective, as ERU for the 2006 growing season (days 160–296) was 4.3 ± 1.1 (Figure 5a), assuming a linear OCS profile, and 3.3 ± 0.6 (Figure 5b), assuming an O_3-shaped OCS profile. Both of these values are lower than the ERU of 5.7 ± 2.1 reported by *Campbell et al.* [2008] for multiple sites in the eastern U.S. However, measured ERU was similar to the relative uptake of OCS over CO_2, approximately 4, calculated from peak-to-peak seasonal differences in OCS and CO_2 measured at Harvard Forest during 2005–2006.

[37] If CO_2 dynamics were controlled by NEE and OCS dynamics were controlled by GPP, at least in part, then a negative y intercept would be expected for a regression between relative OCS and CO_2 gradients. In other words, when the CO_2 gradient is zero (within- and above-canopy CO_2 mole fractions are equal), within-canopy OCS should be lower than above-canopy OCS because the OCS gradient is only influenced by uptake (there is no significant within-canopy OCS source like there is for CO_2). The y intercepts of the regressions were not significantly different from zero (Figure 5). This may be due to the limited number of data points overall, and particularly, the limited number of data points near the beginning and end of the growing season when uptake and gradients were small.

[38] As relative CO_2 uptake becomes small and approaches zero, uncertainty in short-term ERU increases because small changes and/or uncertainty in CO_2 have a large impact. This likely influenced gradient measurements on DOY 166, 173, 272, and 296, where ERU could not be calculated because some gradients were positive. The influence of turbulence also likely influenced the gradients, as strong mixing typically produces a more uniform profile and can lead to near-zero or positive gradients. Thus, the slope of the regression line between relative OCS and CO_2 gradient measurements should provide a better measure of ERU (Figure 5). As a result, growing season ERU should provide a better estimate of GPP_{OCS} as opposed to short-term ERU (Figure 6). However, use of growing season ERU assumes ERU is constant and masks intraseasonal variability, which may arise from variable NEE/GPP or LRU (equation (5)). This study was limited to a few pairs of corresponding CO_2 and OCS gradient measurements, but future studies could potentially benefit from more frequent OCS and CO_2 gradient measurements.

[39] GPP_{OCS} was weakly correlated with GPP_{TER} when short-term ERU values were used to estimate GPP_{OCS}, and uncertainty was approximately 70% of GPP_{OCS} (Figures 6a and 6b). A large fraction of the uncertainty was due to uncertainty in CO_2 gradients, thereby influencing ERU uncertainty, as OCS and CO_2 measurements were not exactly coincident in time; uncertainty in LRU also added significantly to GPP_{OCS} uncertainty. When ERU and LRU uncertainty were halved, GPP_{OCS} uncertainty was reduced to approximately 35%. With different measurement timescales and differing within-canopy CO_2 and OCS measurement heights, short-term ERU values may not be accurate because different air volumes may be measured, leading to differences in GPP_{OCS} and GPP_{TER}.

[40] When growing season ERU (Figure 5) was used to derive GPP_{OCS} from NEE measurements reasonable agreement between GPP_{OCS} and GPP_{TER} was found (Figures 6c and 6d), potentially indicating that errors from extrapolating profiles average out over a season. Potential problems in relating short-term gradients (air samples collected over minutes) to mean fluxes (30 min NEE or GPP; Figures 6a and 6b), such as influence from sweeps/injections of air and/or nonstationarity, are less likely to influence the nominal relationship over a growing season (Figures 6c and 6d). Midday GPP_{OCS} estimates from growing season ERU were higher than GPP_{TER} estimates on average when ERU from the linear OCS profile was used to estimate GPP_{OCS} (Figure 6c; slope of the regression line = 1.28; mean of GPP differences showed GPP_{OCS} was approximately 4% higher than GPP_{TER}), and lower GPP_{TER} when ERU from the O_3-shaped OCS profile was used to estimate GPP_{OCS} (Figure 6c; slope of the regression line = 0.99; mean of GPP differences showed GPP_{OCS} was approximately 3% lower than GPP_{TER}). Total GPP summed over DOY 160–296 showed GPP_{OCS} calculated with ERU = 4.3 matched GPP_{TER} and GPP_{OCS} calculated with ERU = 3.3 was 23% less than GPP_{TER}, but the uncertainty of GPP_{OCS} was approximately 55% of total GPP (Figure 6d). Much of this uncertainty is due to uncertainty in LRU. When LRU uncertainty was halved, from 1.5 to 0.75, GPP_{OCS} uncertainty was reduced to approximately 40% of total GPP. When ERU uncertainty was halved with LRU uncertainty, GPP_{OCS} uncertainty was reduced to approximately 30% of total GPP. When ERU and LRU uncertainty were reduced be two thirds, GPP_{OCS} was approximately 20%, the estimated uncertainty for GPP_{TER}. Previous studies have found that different NEE partitioning methods provide

different estimates of GPP [*Desai et al.*, 2008; *Griffis et al.*, 2004; *Lasslop et al.*, 2010; *Stoy et al.*, 2006]. Differences between GPP_{TER} and GPP_{OCS} estimates may be due to lack of understanding of all ecosystem processes that influence OCS exchange, violation of requirements 1–4 (such as soil OCS uptake), nonconstant ERU and/or LRU, OCS measurement limitations, and/or inaccurate partitioning of NEE via the method of *Reichstein et al.* [2005]. More work needs to be done with OCS in micrometeorological studies to determine if requirements 1–4 are indeed met and if exceptions exist. In future studies, ERU should be calculated from OCS and CO_2 gradient measurements at a colocated sampling position and over the exact same time period.

[41] Ultimately, direct measurement of OCS fluxes via eddy covariance and subsequent estimation of GPP via equation (1) is the best way to use OCS uptake as a GPP proxy. High frequency OCS mole fraction measurements have been made with a quantum cascade laser (QCL) in the laboratory [*Stimler et al.*, 2010b], and show promise, but have not yet been made in the field, thus it is uncertain whether the precision is adequate for eddy covariance. *Stimler et al.* [2010b] reported a 1 Hz measurement precision of 50 pmol mol^{-1} for the QCL; the largest measured OCS difference between the 2.0 and 29.0 m heights in this study was −44 pmol mol^{-1} (linear gradient of −1.6 pmol mol^{-1} m^{-1}), with the smallest difference being near zero and a mean gradient during the 2006 growing season of approximately −0.5 pmol mol^{-1} m^{-1}. Estimated above-canopy (surface layer) OCS gradients were somewhat smaller, which is expected above the canopy, and averaged −0.3 pmol mol^{-1} m^{-1} for the growing season (Figure 7b). These data provide an estimate of the instrument capabilities required to resolve above-canopy gradients in future studies. Given lack of detailed information on OCS within and above vegetation canopies, we cannot use these to confidently predict above-canopy variability in an OCS time series which would be useful to specify requirements for eddy covariance. It is possible that precision may need to improve for eddy covariance. Continuous, fast response measurements are a major advantage provided by laser technology, which is developing rapidly. Instrumentation capable of measuring OCS fluxes via eddy covariance could be used to provide continuous GPP estimates from equation (1), completely independent of NEE measurements.

[42] Estimates of OCS fluxes from GPP_{TER} provide indication of the expected magnitude of vegetation uptake at the flux tower scale, assuming OCS flux is driven by plant uptake, and are also useful for determining OCS measurement requirements. Maximum estimated ecosystem OCS flux at Harvard Forest (approximately −140 pmol m^{-2} s^{-1}; Figure 7a) were similar to maximum fluxes reported by *Xu et al.* [2002] (approximately −140 pmol m^{-2} s^{-1}) for a spruce forest in Germany. Mean fluxes were in the same range, −70 ± 36 pmol m^{-2} s^{-1} at Harvard Forest and −93 ± 12 pmol m^{-2} s^{-1} from *Xu et al.* [2002] for daytime. These OCS flux estimates are one to two orders of magnitude larger than soil uptake fluxes reported in previous studies, which range from approximately 0 to −10 pmol m^{-2} s^{-1} [*Kesselmeier et al.*, 1999; *Kuhn et al.*, 1999; *Liu et al.*, 2010; *Simmons et al.*, 1999; *Steinbacher et al.*, 2004; *White et al.*, 2010; *Xu et al.*, 2002]. If soil fluxes at Harvard Forest were similar to those from previous studies, then OCS flux estimates provide indication that plant uptake was the dominant flux. If other OCS fluxes, such as soil uptake or emission by vegetation [*Berresheim and Vulcan*, 1992], are not negligible compared to vegetation uptake, then ERU measurements or ecosystem-scale flux measurements will contain contributions from these fluxes and will be different than expected if only plants were contributing to uptake, posing problems for using OCS as a GPP proxy.

5.2. Anticipated OCS Gradients at the Additional Sites

[43] Measured CO_2 gradients at the other AmeriFlux sites were correlated to NEE (Table 2 and Figure 8), and projected OCS gradients were correlated to GPP_{TER} (Table 2 and Figure 8). This was expected because OCS gradients were directly projected from CO_2 gradients via an assumed ERU and above-canopy OCS mole fraction, and because GPP_{TER} is closely related to NEE via the NEE partitioning method [*Reichstein et al.*, 2005]. Nonetheless, projected OCS gradients are useful because within-canopy OCS measurements were only made at Harvard Forest in this study, thus projected gradients provide an indication of expected gradients and for determining OCS measurement requirements. Measured and projected OCS gradients plotted versus GPP_{TER} at Harvard Forest showed the slope from measured linear gradients, 0.015 (Figure 4b), was very near the slope from projected gradients, 0.014 (Table 2 and Figure 8, right). This is likely due to the assumed ERU of 4.0, which is near the measured growing season ERU of 4.3 calculated from linear OCS gradients. This provides some confidence that projected OCS gradients at other sites may be a reasonable estimate of actual OCS gradients at those sites, and thus required OCS measurement precision. Estimation of GPP_{OCS} from equation (5) requires accurate measurement of OCS and CO_2 gradients for ERU calculation in equation (4), indicating that the difference measurements required for gradient calculation are more important than absolute accuracy of mole fraction measurements. Thus measurement precision is more important than absolute accuracy using the ERU approach for estimating GPP_{OCS}.

[44] At the other forest sites, projected OCS gradients were similar to the measured gradients, estimated surface layer gradients, and projected gradients at Harvard Forest (Table 3 and Figures 7b and 8). Maximum projected OCS gradients (largest negative values) at forest sites were comparable to current uncertainty in OCS measurement capabilities, approximately 0.5% (S. Montzka, unpublished data, 2010), which yields 1.5–2.8 pmol mol^{-1} for OCS mole fractions ranging from 300 to 550 pmol mol^{-1}. However, other issues may affect the ability to discern small differences from flask samples, namely the potential of artifacts associated with sample storage and contamination. Despite challenges with flask sample measurements, results at Harvard Forest indicate ERU can be measured (Figure 5), suggesting ERU is potentially measurable at other forest sites, particularly with the potential of high frequency, in situ measurements that can be averaged over longer time periods [*Stimler et al.*, 2010b]. It is possible that OCS gradients at Harvard Forest were measurable because within-canopy OCS was measured near the soil surface at 2.0 m. If the entire canopy acted as an OCS sink, as has been suggested by previous studies where OCS profiles were measured [*Mihalopoulos et al.*, 1989; *Mihalopoulos and Nguyen*, 2001; *White et al.*, 2010], the

lowest OCS mole fractions would likely occur near the soil surface. It may be that OCS gradients would be difficult to measure at the same within-canopy height as CO_2 gradients due to OCS measurement limitations, but the previous studies where OCS profiles were measured provide some optimism. It should be noted that measured CO_2 gradients, and as a result the corresponding projected OCS gradients, were positive some of the time for all sites (Table 3 and Figure 8), indicating that within-canopy CO_2 uptake was sometimes outweighed by respiratory release, affected by mixing, and/or influenced by urban pollution. Positive values of projected OCS gradients calculated from measured CO_2 gradients are strictly a result of calculation from equations (2)–(4). It is not anticipated that positive OCS gradients will always correspond to positive CO_2 gradients when actual OCS measurements are used for gradient calculation.

[45] Projected OCS gradients in short canopies (C_4 grassland and soybean crop) were much greater than projected gradients in taller forest canopies for a given GPP (Table 3 and Figure 8), with maximum values greater than current uncertainty in OCS measurement capabilities. In light of the encouraging results from Harvard Forest reported herein, OCS measurements and resulting GPP_{OCS} estimates may be even more useful in short canopies. One of the main differences between grassland or cropped agricultural ecosystems and forests is canopy height and structure, where photosynthesizing leaf area is contained within a small volume in grassland and agricultural ecosystems compared to forests. Even if forest canopies and shorter canopies have similar leaf area, it is spread over a much larger volume in forests, thus gradients are likely to be much smaller in forests than in short canopies, assuming similar NEE and GPP rates (Figure 8). Additionally, mixing is often enhanced in forests relative to short canopies due to the aerodynamic roughness and relative openness of forest canopies. These distinctions are illustrated by comparing measured CO_2 and projected OCS gradients at Kendall Grassland and Niwot Ridge, which had similar NEE and GPP_{TER} rates (approximately -10 to -15 μmol m^{-2} s^{-1}, respectively) during the growing season. CO_2 gradients and OCS gradients were much larger in the grassland relative to the forest. On average, measured CO_2 gradients at Kendall grassland were approximately 9 times greater than the measured CO_2 gradients at Niwot Ridge (Table 3), even with a lower leaf area index at Kendall Grassland (Table 1), resulting in projected OCS gradients at Kendall Grassland that were approximately 9 times greater than those at Niwot Ridge.

6. Conclusions

[46] Prior studies have indicated the possibility of using OCS uptake as a GPP proxy. Clearly, GPP estimation via NEE partitioning from OCS measurements (equation (5)) requires reduced uncertainty in ERU and LRU. Despite shortcomings in the OCS measurements (within-canopy CO_2 and OCS measurements were not colocated, within- and above-canopy OCS mole fraction measurements and CO_2 and OCS mole fraction measurements were not exactly coincident in time), estimates of GPP scaled from NEE measurements using measured ERU and estimated LRU produced results similar to a standard and widely applied NEE partitioning method for GPP estimation [*Reichstein et al.*, 2005]. This demonstrates potential utility of OCS in constraining GPP in micrometeorological studies, particularly as higher frequency and higher resolution OCS measurement instrumentation becomes available.

[47] Given the need for accurate partitioning of NEE measurements into component fluxes, further studies of OCS uptake as a GPP proxy are warranted. More work is required to determine whether requirements 1–4 are met at flux tower sites and whether exceptions exist at different sites. Specifically, characterization of plant OCS uptake relative to other ecosystem fluxes, namely soil exchange and the possibility of plant emission, is required. Leaf level studies provide strong indication that the requirements 1–4 are met, but most leaf level studies have been performed under controlled conditions. An important next step toward using OCS uptake as a GPP proxy at the flux tower scale is to further study OCS dynamics and exchange in various ecosystems. Specifically, better characterization of LRU variability is required, in addition to concurrent, colocated OCS and CO_2 above-canopy profile measurements and/or direct OCS flux measurements, which allow GPP estimation and comparison to GPP estimates from currently applied NEE partitioning techniques. Investigations in short-statured canopies are likely to provide the most information in the near term, while analytical instruments continue to improve.

[48] **Acknowledgments.** Thanks to Elaine Gottlieb for help in collecting the within-canopy OCS samples at Harvard Forest; John Baker, Sean Burns, Ken Davis, and Hans-Peter Schmid for sharing AmeriFlux data; John Miller for thoughtful ideas and discussion; Tom Boden and the CDIAC staff for maintaining the AmeriFlux data archive; Markus Reichstein for maintaining the flux data gap-filling and flux-partitioning website; and Ryan Campbell for reviewing an early version of the paper. This research was supported by the Office of Science (BER), U.S. Department of Energy, grant DE-SC0005236. Any opinions, findings, and conclusions or recommendations expressed in this publication are those of the authors and do not necessarily reflect the views of the DOE. Mark Blonquist gratefully acknowledges support from the National Science Foundation Division of Graduate Education, grant DGE08–41233, and the University of Utah. OCS measurements were supported in part by the Atmospheric Composition and Climate Program of the National Oceanic and Atmospheric Administration's Climate Program Office. Observations at Harvard Forest were supported by the Office of Science (BER), U.S. Department of Energy, grant DE-FG02-07ER64358, and through the Northeastern Regional Center of the National Institute for Climate Change Research (3452-HU-DOE-4157). Observations at Morgan Monroe State Forest were supported by the Office of Science (BER), U.S. Department of Energy, through the Midwestern Center of the National Institute for Global Environmental Change (NIGEC), grant DE-FC03-90ER61010, and from BER, grant DE-FG02-07ER64371. Observations at Willow Creek were supported by the Office of Science (BER), U.S. Department of Energy, through the Midwestern Regional Center of the National Institute for Global Environmental Change, under Cooperative Agreement No. DE-FC03-90ER61010, and USDA Northern Research Station Joint Venture, agreement 09-JV-11242306-105, and the Wisconsin Focus on Energy. Observations at Niwot Ridge were supported by the Western Section of the National Institute for Climate Change Research (NICCR), which was supported by the Office of Biological Research at the Department of Energy, and the Long-Term Research in Environmental Biology (LTREB) Program at the National Science Foundation. Observations at Kendall Grassland were supported by USDA-ARS. Observations at Rosemount were supported by the National Science Foundation, grant ATM-0546476, and the Office of Science (BER), U.S. Department of Energy, grant DE-FG02-06ER64316.

References

Baldocchi, D. D., and K. B. Wilson (2001), Modeling CO_2 and water vapor exchange of a temperature broadleaved forest across hourly to decadal time scales, *Ecol. Modell.*, *142*, 155–184, doi:10.1016/S0304-3800(01)00287-3.

Baldocchi, D., et al. (2001), FLUXNET: A new tool to study the temporal and spatial variability of ecosystem-scale carbon dioxide, water vapor,

and energy flux densities, *Bull. Am. Meteorol. Soc.*, *82*, 2415–2434, doi:10.1175/1520-0477(2001)082<2415:FANTTS>2.3.CO;2.

Bartell, U., U. Hofmann, R. Hofmann, B. Kreuzburg, M. O. Andreae, and J. Kesselmeier (1993), COS and H_2S fluxes over a wet meadow in relation to photosynthetic activity: An analysis of measurements made on 6 September 1990, *Atmos. Environ.*, *27A*, 1851–1864.

Berresheim, H., and V. D. Vulcan (1992), Vertical distributions of COS, CS_2, DMS and other sulfur compounds in a loblolly pine forest, *Atmos. Environ.*, *26A*, 2031–2036.

Blake, N. J., et al. (2008), Carbonyl sulfide (OCS): Large-scale distributions over North America during INTEX-NA and relationship to CO_2, *J. Geophys. Res.*, *113*, D09S90, doi:10.1029/2007JD009163.

Brown, K. A., and J. N. B. Bell (1986), Vegetation—The missing sink in the global cycle of carbonyl sulfide (COS), *Atmos. Environ.*, *20*, 537–540, doi:10.1016/0004-6981(86)90094-6.

Caird, M. A., J. H. Richards, and L. A. Donovan (2007), Nighttime stomatal conductance and transpiration in C_3 and C_4 plants, *Plant Physiol.*, *143*, 4–10, doi:10.1104/pp.106.092940.

Campbell, J. E., et al. (2008), Photosynthetic control of atmospheric carbonyl sulfide during the growing season, *Science*, *322*, 1085–1088, doi:10.1126/science.1164015.

Castro, M. S., and J. N. Galloway (1991), A comparison of sulfur-free and ambient air enclosure techniques for measuring the exchange of reduced sulfur gases between soils and the atmosphere, *J. Geophys. Res.*, *96*(D8), 15,427–15,437, doi:10.1029/91JD01399.

Cellier, P., and Y. Brunet (1992), Flux-gradient relationships above tall plant canopies, *Agric. For. Meteorol.*, *58*, 93–117, doi:10.1016/0168-1923(92)90113-I.

Cook, B. D., et al. (2004), Carbon exchange and venting anomalies in an upland deciduous forest in northern Wisconsin, USA, *Agric. For. Meteorol.*, *126*, 271–295, doi:10.1016/j.agrformet.2004.06.008.

Denmead, O. T., and E. F. Bradley (1985), Flux-gradient relationships in a forest canopy, in *The Forest-Atmosphere Interaction*, edited by B. A. Hutchinson and B. B. Hicks, pp. 421–442, Reidel, Norwell, Mass.

Desai, A. R., et al. (2008), Cross-site evaluation of eddy covariance GPP and RE decomposition techniques, *Agric. For. Meteorol.*, *148*, 821–838, doi:10.1016/j.agrformet.2007.11.012.

Geng, C., and Y. Mu (2004), Carbonyl sulfide and dimethyl sulfide exchange between lawn and the atmosphere, *J. Geophys. Res.*, *109*, D12302, doi:10.1029/2003JD004492.

Gillon, J. S., and D. Yakir (2000), Naturally low carbonic anhydrase activity in C_4 and C_3 plants limits discrimination against $C^{18}OO$ during photosynthesis, *Plant Cell Environ.*, *23*, 903–915, doi:10.1046/j.1365-3040.2000.00597.x.

Goldan, P. D., R. Fall, W. C. Kuster, and F. C. Fehsenfeld (1988), Uptake of OCS by growing vegetation: A major tropospheric sink, *J. Geophys. Res.*, *93*, 14,186–14,192, doi:10.1029/JD093iD11p14186.

Goldstein, A. H., M. McKay, M. R. Kurpius, G. W. Schade, A. Lee, R. Holzinger, and R. A. Rasmussen (2004), Forest thinning experiment confirms ozone deposition to a forest canopy is dominated by reaction with biogenic VOCs, *Geophys. Res. Lett.*, *31*, L22106, doi:10.1029/2004GL021259.

Goulden, M. L., J. W. Munger, S.-M. Fan, B. C. Daube, and S. C. Wofsy (1996), Measurements of carbon sequestration by long-term eddy covariance: Methods and a critical evaluation of accuracy, *Global Change Biol.*, *2*, 169–182, doi:10.1111/j.1365-2486.1996.tb00070.x.

Griffis, T. J., T. A. Black, D. Gaumont-Guay, G. B. Drewitt, Z. Nesic, A. G. Barr, K. Morgenstern, and N. Kljun (2004), Seasonal variation and partitioning of ecosystem respiration in a southern boreal aspen forest, *Agric. For. Meteorol.*, *125*, 207–223, doi:10.1016/j.agrformet.2004.04.006.

Griffis, T. J., J. M. Baker, and J. Zhang (2005), Seasonal dynamics and partitioning of isotopic CO_2 exchange in a C_3/C_4 managed ecosystem, *Agric. For. Meteorol.*, *132*, 1–19, doi:10.1016/j.agrformet.2005.06.005.

Horii, C. V., J. W. Munger, and S. C. Wofsy (2004), Fluxes of nitrogen oxides over a temperate deciduous forest, *J. Geophys. Res.*, *109*, D08305, doi:10.1029/2003JD004326.

Kesselmeier, J., and A. Hubert (2002), Exchange of reduced volatile sulfur compounds between leaf litter and the atmosphere, *Atmos. Environ.*, *36*, 4679–4686, doi:10.1016/S1352-2310(02)00413-2.

Kesselmeier, J., and L. Merk (1993), Exchange of carbonyl sulfide (COS) between agricultural plants and the atmosphere: Studies on the deposition of COS to peas, corn, and rapeseed, *Biogeochemistry*, *23*, 47–59, doi:10.1007/BF00002922.

Kesselmeier, J., N. Teusch, and U. Kuhn (1999), Controlling variables for the uptake of atmospheric carbonyl sulfide by soil, *J. Geophys. Res.*, *104*, 11,577–11,584, doi:10.1029/1999JD900090.

Kettle, A. J., U. Kuhn, M. von Hobe, J. Kesselmeier, and M. O. Andreae (2002), Global budget of atmospheric carbonyl sulfide: Temporal and spatial variations of the dominant sources and sinks, *J. Geophys. Res.*, *107*(D22), 4658, doi:10.1029/2002JD002187.

Kluczewski, S. M., K. A. Brown, and J. N. B. Bell (1985), Deposition of [^{35}S]-carbonyl sulphide to vegetable crops, *Radiat. Prot. Dosimetry*, *11*, 173–177.

Kuhn, U., C. Ammann, A. Wolf, F. X. Meixner, M. O. Andreae, and J. Kesselmeier (1999), Carbonyl sulfide exchange on an ecosystem scale: Soil represents a dominant sink for atmospheric COS, *Atmos. Environ.*, *33*, 995–1008, doi:10.1016/S1352-2310(98)00211-8.

Kurpius, M. R., and A. H. Goldstein (2003), Gas-phase chemistry dominates O_3 loss to a forest, implying a source of aerosols and hydroxyl radicals to the atmosphere, *Geophys. Res. Lett.*, *30*(7), 1371, doi:10.1029/2002GL016785.

Lasslop, G., M. Reichstein, D. Papale, A. D. Richardson, A. Arneth, A. Barr, P. Stoy, and G. Wohlfahrt (2010), Separation of net ecosystem exchange into assimilation and respiration using a light response curve approach: Critical issues and global evaluation, *Global Change Biol.*, *16*, 187–208, doi:10.1111/j.1365-2486.2009.02041.x.

Lavigne, M. B., et al. (1997), Comparing nocturnal eddy covariance measurements to estimates of ecosystem respiration made by scaling chamber measurements at six coniferous boreal sites, *J. Geophys. Res.*, *102*, 28,977–28,985, doi:10.1029/97JD01173.

Law, B. E., M. G. Ryan, and P. M. Anthoni (1999), Seasonal and annual respiration of a Ponderosa pine ecosystem, *Global Change Biol.*, *5*, 169–182, doi:10.1046/j.1365-2486.1999.00214.x.

Liu, J., C. Geng, Y. Mu, Y. Zhang, Z. Xu, and H. Wu (2010), Exchange of carbonyl sulfide (COS) between the atmosphere and various soils in China, *Biogeosciences*, *7*, 753–762, doi:10.5194/bg-7-753-2010.

Mihalopoulos, N., and B. C. Nguyen (2001), Vertical distribution of carbonyl sulfide in a eucalyptus forest, *Chemosphere Global Change Sci.*, *3*, 275–282, doi:10.1016/S1465-9972(01)00010-1.

Mihalopoulos, N., B. Bonsang, B. C. Nguyen, M. Kanakidou, and S. Belviso (1989), Field observations of carbonyl sulfide deficit near the ground: Possible implication of vegetation, *Atmos. Environ.*, *23*, 2159–2166, doi:10.1016/004-6981(89)90177-7.

Monson, R. K., A. A. Turnipseed, J. P. Sparks, P. C. Harley, L. E. Scott-Denton, K. Sparks, and T. E. Huxman (2002), Carbon sequestration in a high-elevation, subalpine forest, *Global Change Biol.*, *8*, 459–478, doi:10.1046/j.1365-2486.2002.00480.x.

Montzka, S. A., and P. P. Tans (2004), Can carbonyl sulfide help constrain gross vegetative fluxes of carbon dioxide?, *EOS Trans. AGU*, *85*(47), Fall Meet. Suppl., Abstract B21E–04.

Montzka, S. A., M. Aydin, M. Battle, J. H. Butler, E. S. Saltzman, B. D. Hall, A. D. Clarke, D. Mondeel, and J. W. Elkins (2004), A 350-year atmospheric history for carbonyl sulfide inferred from Antarctic firn air and air trapped in ice, *J. Geophys. Res.*, *109*, D22302, doi:10.1029/2004JD004686.

Montzka, S. A., P. Calvert, B. D. Hall, J. W. Elkins, T. J. Conway, P. P. Tans, and C. Sweeney (2007), On the global distribution, seasonality, and budget of atmospheric carbonyl sulfide (COS) and some similarities to CO_2, *J. Geophys. Res.*, *112*, D09302, doi:10.1029/2006JD007665.

Munger, J. W., S. C. Wofsy, P. S. Bakwin, S.-M. Fan, M. L. Goulden, B. C. Daube, A. H. Goldstein, K. E. Moore, and D. R. Fitzjarrald (1996), Atmospheric deposition of reactive nitrous oxides and ozone in a temperate deciduous forest and a subarctic woodland: 1. Measurements and mechanisms, *J. Geophys. Res.*, *101*, 12,639–12,657, doi:10.1029/96JD00230.

Munger, J. W., S.-M. Fan, P. S. Bakwin, M. L. Goulden, A. H. Goldstein, A. S. Colman, and S. C. Wofsy (1998), Regional budgets for nitrogen oxides from continental sources: Variations of rates for oxidation and deposition with season and distance from source region, *J. Geophys. Res.*, *103*, 8355–8368, doi:10.1029/98JD00168.

Notni, J., S. Schenk, G. Protoschill-Krebs, J. Kesselmeier, and E. Anders (2007), The missing link in COS metabolism: Study on the reactivation of carbonic anhydrase from its hydrosulfide analogue, *ChemBioChem*, *8*, 530–536, doi:10.1002/cbic.200600436.

Ogée, J., Y. Brunet, P. Loustau, P. Berbigier, and S. Delzon (2003a), *MuSICA*, a CO_2, water and energy multilayer, multileaf pine forest model: Evaluation from hourly to yearly time scales and sensitivity analysis, *Global Change Biol.*, *9*, 697–717, doi:10.1046/j.1365-2486.2003.00628.x.

Ogée, J., P. Peylin, P. Ciais, T. Bariac, Y. Brunet, P. Berbigier, C. Roche, P. Richard, G. Bardoux, and J.-M. Bonnefond (2003b), Partitioning net ecosystem carbon exchange into net assimilation and respiration using $^{13}CO_2$ measurements: A cost-effective sampling strategy, *Global Biogeochem. Cycles*, *17*(2), 1070, doi:10.1029/2002GB001995.

Ogée, J., P. Peylin, M. Cuntz, T. Bariac, Y. Brunet, P. Berbigier, P. Richard, and P. Ciais (2004), Partitioning net ecosystem carbon exchange into net assimilation and respiration with canopy-scale isotopic

measurements: An error propagation analysis with $^{13}CO_2$ and $CO^{18}O$ data, *Global Biogeochem. Cycles*, *18*, GB2019, doi:10.1029/2003GB002166.

Protoschill-Krebs, G., and J. Kesselmeier (1992), Enzymatic pathways for the metabolization of carbonyl sulphide (COS) by higher plants, *Bot. Acta*, *108*, 445–448.

Protoschill-Krebs, G., C. Wilhelm, and J. Kesselmeier (1996), Consumption of carbonyl sulphide (COS) by higher plant carbonic anhydrase (CA), *Atmos. Environ.*, *30*(18), 3151–3156.

Puxbaum, H., and G. König (1997), Observation of dipropenyldisulfide and other organic sulfur compounds in the atmosphere of a beech forest with *Allium ursinum* ground cover, *Atmos. Environ.*, *31*, 291–294, doi:10.1016/1352-2310(96)00162-8.

Raupach, M. R. (1979), Anomalies in flux-gradient relationships over forest, *Boundary Layer Meteorol.*, *16*, 467–486, doi:10.1007/BF03163564.

Reichstein, M., et al. (2005), On the separation of net ecosystem exchange into assimilation and ecosystem respiration: Review and improved algorithm, *Global Change Biol.*, *11*, 1424–1439, doi:10.1111/j.1365-2486.2005.001002.x.

Richardson, A. D., et al. (2006), A multi-site analysis of random error in tower-based measurements of carbon and energy fluxes, *Agric. For. Meteorol.*, *136*, 1–18, doi:10.1016/j.agrformet.2006.01.007.

Sacks, W. J., D. S. Schimel, and R. K. Monson (2007), Coupling between carbon cycling and climate in a high-elevation, subalpine forest: A model-data fusion analysis, *Oecologia*, *151*, 54–68, doi:10.1007/s00442-006-0565-2.

Sandoval-Soto, L., M. Stanimirov, M. von Hobe, V. Schmitt, J. Valdes, A. Wild, and J. Kesselmeier (2005), Global uptake of carbonyl sulfide (COS) by terrestrial vegetation: Estimates corrected by deposition velocities normalized to the uptake of carbon dioxide (CO_2), *Biogeosciences*, *2*, 125–132, doi:10.5194/bg-2-125-2005.

Scanlon, T. M., and W. P. Kustas (2010), Partitioning water vapor and carbon dioxide fluxes using correlation analysis, *Agric. For. Meteorol.*, *150*, 89–99, doi:10.1016/j.agrformet.2009.09.005.

Schmid, H. P., C. S. B. Grimmond, F. Cropley, B. Offerle, and H.-B. Su (2000), Measurements of CO_2 and energy fluxes over a mixed hardwood forest in the mid-western United States, *Agric. For. Meteorol.*, *103*, 357–374, doi:10.1016/S0168-1923(00)00140-4.

Scott, R. L., E. P. Hamerlynck, G. D. Jenerette, M. S. Moran, and G. Barron-Gafford (2010), Carbon dioxide exchange in a semidesert grassland through drought-induced vegetation change, *J. Geophys. Res.*, *115*, G03026, doi:10.1029/2010JG001348.

Seibt, U., J. Kesselmeier, L. Sandoval-Soto, U. Kuhn, and J. A. Berry (2010), A kinetic analysis of leaf uptake of COS and its relation to transpiration, photosynthesis, and carbon isotope fractionation, *Biogeosciences*, *7*, 333–341, doi:10.5194/bg-7-333-2010.

Simmons, J. S., L. Klemedtsson, H. Hultberg, and M. E. Hines (1999), Consumption of atmospheric carbonyl sulfide by coniferous boreal forest soils, *J. Geophys. Res.*, *104*, 11,569–11,576, doi:10.1029/1999JD900149.

Steinbacher, M., H. G. Bingemer, and U. Schmidt (2004), Measurements of the exchange of carbonyl sulfide (OCS) and carbon disulfide (CS_2) between soil and atmosphere in a spruce forest in central Germany, *Atmos. Environ.*, *38*, 6043–6052, doi:10.1016/j.atmosenv.2004.06.022.

Stimler, K., S. A. Montzka, J. A. Berry, Y. Rudich, and D. Yakir (2010a), Relationships between carbonyl sulfide (COS) and CO_2 during leaf gas exchange, *New Phytol.*, *186*, 869–878, doi:10.1111/j.1469-8137.2010.03218.x.

Stimler, K., D. Nelson, and D. Yakir (2010b), High precision measurements of atmospheric concentrations and plant exchange rates of carbonyl sulfide using mid-IR quantum cascade laser, *Global Change Biol.*, *16*, 2496–2503, doi:10.1111/j.1365-2486.2009.02088.x.

Stoy, P. C., G. G. Katul, M. B. S. Sequeira, J. Y. Juang, K. A. Novick, J. M. Uebelherr, and R. Oren (2006), An evaluation of models for partitioning eddy covariance-measured net ecosystem exchange into photosynthesis and respiration, *Agric. For. Meteorol.*, *141*, 2–18, doi:10.1016/j.agrformet.2006.09.001.

Suntharalingam, P., A. J. Kettle, S. M. Montzka, and D. J. Jacob (2008), Global 3-D model analysis of seasonal cycle of atmospheric carbonyl sulfide: Implications for terrestrial vegetation uptake, *Geophys. Res. Lett.*, *35*, L19801, doi:10.1029/2008GL034332.

Taylor, J. R. (1997), *An Introduction to Error Analysis: The Study of Uncertainties in Physical Measurements*, Univ. Sci. Books, Sausalito, Calif.

Turnipseed, A. A., S. P. Burns, D. J. P. Moore, J. Hu, A. B. Guenther, and R. K. Monson (2009), Controls over ozone deposition to a high elevation subalpine forest, *Agric. For. Meteorol.*, *149*, 1447–1459, doi:10.1016/j.agrformet.2009.04.001.

Urbanski, S., C. Barford, S. Wofsy, C. Kucharik, E. Pyle, J. Budney, K. McKain, D. Fitzjarrald, M. Czikowsky, and J. W. Munger (2007), Factors controlling CO_2 exchange on timescales from hourly to decadal at Harvard Forest, *J. Geophys. Res.*, *112*, G02020, doi:10.1029/2006JG000293.

Van Diest, H., and J. Kesselmeier (2008), Soil atmosphere exchange of carbonyl sulfide (COS) regulated by diffusivity depending on water-filled pore space, *Biogeosciences*, *5*, 475–483, doi:10.5194/bg-5-475-2008.

van Gorsel, E., et al. (2009), Estimating nocturnal ecosystem respiration from the vertical turbulent flux and change in storage of CO_2, *Agric. For. Meteorol.*, *149*, 1919–1930, doi:10.1016/j.agrformet.2009.06.020.

Watts, S. F. (2000), The mass budgets of carbonyl sulfide, dimethyl sulfide, carbon disulfide and hydrogen sulfide, *Atmos. Environ.*, *34*, 761–779, doi:10.1016/S1352-2310(99)00342-8.

White, M. L., Y. Zhou, R. S. Russo, H. Mao, R. Talbot, R. K. Varner, and B. C. Sive (2010), Carbonyl sulfide exchange in a temperate loblolly pine forest grown under ambient and elevated CO_2, *Atmos. Chem. Phys.*, *10*, 547–561, doi:10.5194/acp-10-547-2010.

Wingate, L., et al. (2009), The impact of soil microorganisms on the global budget of $\delta^{18}O$ in atmospheric CO_2, *Proc. Natl. Acad. Sci. U. S. A.*, *106*, 22,411–22,415, doi:10.1073/pnas.0905210106.

Wyngaard, J. C. (2010), *Turbulence in the Atmosphere*, Cambridge Univ. Press, New York, doi:10.1017/CBO9780511840524.

Xu, X., H. G. Bingemer, and U. Schmidt (2002), The flux of carbonyl sulfide and carbon disulfide between the atmosphere and a spruce forest, *Atmos. Chem. Phys.*, *2*, 171–181, doi:10.5194/acp-2-171-2002.

Yi, C., et al. (2004), A nonparametric method for separating photosynthesis and respiration components in CO_2 flux measurements, *Geophys. Res. Lett.*, *31*, L17107, doi:10.1029/2004GL020490.

Yonemura, S., L. Sandoval-Soto, J. Kesselmeier, U. Kuhn, M. von Hobe, D. Yakir, and S. Kawahima (2005), Uptake of carbonyl sulfide (COS) and emissions of dimethyl sulfide (DMS) by plants, *Phyton*, *45*, 17–24.

Zha, T., Z. Xing, K.-Y. Wang, S. Kellomäki, and A. G. Barr (2007), Total and component carbon fluxes of a Scots pine ecosystem from chamber measurements and eddy covariance, *Ann. Bot.*, *99*, 345–353, doi:10.1093/aob/mcl266.

Zobitz, J. M., S. P. Burns, M. Reichstein, and D. R. Bowling (2008), Partitioning net ecosystem carbon exchange and the carbon isotopic disequilibrium in a subalpine forest, *Global Change Biol.*, *14*, 1785–1800, doi:10.1111/j.1365-2486.2008.01609.x.

J. M. Blonquist Jr. and D. R. Bowling, Department of Biology, University of Utah, 257 S. 1400 E, Salt Lake City, UT 84112, USA. (mark.blonquist@utah.edu)

A. R. Desai, Department of Atmospheric and Oceanic Sciences, University of Wisconsin-Madison, 1225 W. Dayton St., AOSS 1549, Madison, WI 53706, USA.

D. Dragoni, Department of Geography, Indiana University, 701 E. Kirkwood Ave., Bloomington, IN 47405, USA.

T. J. Griffis, Department of Soil, Water, and Climate, University of Minnesota-Twin Cities, 1991 Upper Buford Cir., Soil Science Rm. 331, St. Paul, MN 55108, USA.

R. K. Monson, Department of Ecology and Evolutionary Biology, University of Colorado at Boulder, Boulder, CO 80309, USA.

S. A. Montzka, Global Monitoring Division, NOAA Earth System Research Laboratory, 325 Broadway, Boulder, CO 80305-3328, USA.

J. W. Munger, Department of Earth and Planetary Sciences, Harvard University, 20 Oxford St., Cambridge, MA 02138, USA.

R. L. Scott, Southwest Watershed Research Center, USDA ARS, 2000 E. Allen Rd., Tucson, AZ 85719, USA.

D. Yakir, Department of Environmental Sciences and Energy Research, Weizmann Institute of Science, Rehovot 76100, Israel.